Engineering Structures 298 (2024) 117046

Contents lists available at ScienceDirect

Engineering Structures

journal homepage: www.elsevier.com/locate/engstruct

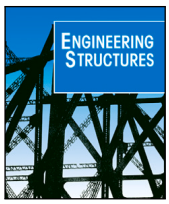

An efficient automatic modal identification method based on free vibration response and enhanced Empirical Fourier Decomposition technique

Matteo Mazzeo [a], Dario De Domenico [a,*], Giuseppe Quaranta [b], Roberta Santoro [a]

[a] Department of Engineering, University of Messina, Contrada Di Dio, 98166 Sant'Agata, Messina, Italy
[b] Department of Structural and Geotechnical Engineering, Sapienza University of Rome, Via Eudossiana 18, 00184 Rome, Italy

ARTICLE INFO

Keywords:
Bridge
Cable
Damping
Empirical Fourier Decomposition
Free vibration
Identification
Variational Mode Decomposition

ABSTRACT

This paper presents an efficient yet practical approach for the automatic modal identification of structures based on their free vibration response. The proposed approach relies on the Empirical Fourier Decomposition (EFD) technique. It implements a new procedure to recognize automatically the number of modal components to be extracted from noisy data in such a way to prevent both mode-mixing and mode-splitting effects. A suitable strategy is adopted to improve the segmentation of the frequency spectrum of the free vibration response, so as to identify accurately the bounds of the frequency spectrum partition corresponding to each modal component. The related modal damping ratios are estimated by means of a robust area-based approach in order to mitigate the noise-induced disturbances whereas a time-domain method based on the phase shift of the free vibration response peaks is employed to identify the mode shapes.

The proposed approach is first validated through the analysis of synthetic signals that embed closely spaced components and a lowly excited vibration mode. Finally, the proposed approach is applied to two real bridges. The first case-study deals with the identification of modal frequencies and damping ratios of the cables of a stay-cabled bridge. The second case-study involves the modal identification of a steel railway bridge deck that exhibits two closely spaced vibration modes. The outcomes obtained using the proposed approach based on EFD technique are compared with the results obtained by means of the Variational Mode Decomposition (VMD) technique as well as with those computed through classical operational modal analysis techniques. The consistent estimates produced by means of the proposed approach demonstrate its accuracy and robustness.

1. Introduction

The dynamic identification of the modal parameters is an effective nondestructive way to assess the condition of an existing structure. Indeed, the modal parameters that can be identified from the dynamic response are strictly related to essential, physical features of the structure such as mass, stiffness and energy dissipation. Therefore, they can be conveniently used to monitor the global structural behavior while their variation in time might serve at detecting and tracking damage. The estimation of modal frequencies, damping ratios and mode shapes thus plays a crucial role for structural model updating [1] and diagnostic [2]. Nonetheless, while the installation of large permanent sensor networks is becoming popular for the continuous dynamic identification of major structures from ambient response, there exists a large number of constructions that can only be monitored sporadically and in a short time because of budget, technical and practical constraints. In such a case, free vibration tests might be a suitable strategy for dynamic identification because they can be performed by means of a network consisting of a few sensors temporarily installed on the structure in such a way to limit duration and cost of the experimental campaign. Additionally, free vibration tests are usually performed by introducing an initial perturbation that can induce a response significantly higher than the ambient response. This, in turn, allows to reduce the noise-to-signal ratio in the final measurements and/or to consider less stringent requirements about the technical specifications of the sensors. The results obtained from the free decay of the dynamic response are thus generally recognized to be more accurate because the influence of the noise is smaller and there is no need to make assumptions about the loading conditions [3].

Several free vibration tests have been performed for the experimental dynamic characterization of base-isolated buildings [4–6], high-rise buildings [7], masonry towers [8] and ancient tie-rods [9,10]. Free vibration tests are also very common for the dynamic identification of the modal features of some bridge typologies and components. Depending on how the free response is induced and/or which component of the bridge is tested, it might require a temporary closure of the infrastructure and the corresponding authorization by deputed authorities.

* Corresponding author.
E-mail address: dario.dedomenico@unime.it (D. De Domenico).

https://doi.org/10.1016/j.engstruct.2023.117046
Received 27 April 2023; Received in revised form 23 September 2023; Accepted 13 October 2023
Available online 31 October 2023
0141-0296/© 2023 The Authors. Published by Elsevier Ltd. This is an open access article under the CC BY-NC-ND license (http://creativecommons.org/licenses/by-nc-nd/4.0/).

In order to alleviate these practical issues, free vibration tests can be arranged together with other activities that require a temporary bridge closure, such as exceptional maintenance or retrofitting interventions, static tests or inspections following accidental extreme events. Actually, most of the existing applications of free vibration tests for modal identification are related to bridges. For example, Cunha et al. [11] have performed free vibration tests to estimate the modal damping ratios of a cable-stayed bridge. The free vibrations for this test have been obtained by releasing a barge attached by means of a cable. Similarly, Magalhães et al. [12] have performed the dynamic identification of a bridge deck by exploiting its free vibrations due to the sudden rupture of a cable with an attached heavy counterweight. The free vibrations following the passage of a train have been often elaborated for the dynamic identification of railway bridges [13,14]. Ko et al. [15] have identified the equivalent damping of bridge stay cables equipped with a magnetorheological damper from the free vibration decay following a sinusoidal excitation. Van Nimmen et al. [16] estimated the equivalent damping of a footbridge equipped with a tuned mass damper from its free decay response induced by one person bobbing at the midspan.

The identification of the modal parameters through the elaboration of the free response of a structure is generally accomplished by detecting and extracting its uni-modal components from the recorded vibrations. Several decomposition techniques have been proposed in the last decades for this task. One of the most common is the Empirical Mode Decomposition (EMD) technique [17], which combines an iterative sifting process and the Hilbert–Huang transform. Despite its widespread use, however, several studies have shown that the EMD technique and, to a less extent, its improved variants [18] suffer from mode-mixing effects [19,20]. Another approach based on the Hilbert theory is the Hilbert Vibration Decomposition (HVD) technique [21]. An adaptive decomposition method based on wavelet analysis is the Empirical Wavelet Transform (EWT) [22], which adopts a particular form for the wavelet basis. The EWT initially operates a segmentation of the frequency spectrum and a wavelet filter bank is next applied to each segment to extract the uni-modal components. This method has also some drawbacks: in fact, if the signal to be decomposed has a high noise-to-signal ratio, then trivial (i.e., non-physical) components might be extracted, thereby leading to gross errors [23]. Furthermore, the transition phase related to each filter in the bank may produce interference between contiguous uni-modal components, especially in case of closely spaced modes, thus originating mode-mixing phenomena [24]. Another adaptive decomposition technique is the Fourier Decomposition Method (FDM) [25], which combines Fourier theory and Hilbert transform to decompose the signal into a set of Fourier intrinsic band functions. The main limitations of the FDM are attributable to the poor performance in decomposing signals with low spectral resolution or with closely spaced spectral components [26]. An adaptive decomposition method based on a variational formulation is the Variational Modal Decomposition (VMD) technique [27], which relies on a solid mathematical basis that differs significantly from all existing proposals. In fact, it achieves the signal decomposition within a computational framework in which the bandwidth associated to each component is assessed by searching for the optimal solution of a constrained variational problem. A very recent decomposition method is the Empirical Fourier Decomposition (EFD) technique [24], which operates the uni-modal components extraction via an improved suitable segmentation of the frequency spectrum and a zero-phase filter bank.

The VMD technique and the EFD technique are among the approaches that are fast attracting more and more attention in this field. One of the first applications of the VMD technique in structural dynamic identification has been reported by Bagheri et al. [28], who have adopted such a method to identify the modal parameters of a footbridge. Civera and Surace [29] have analyzed pros and cons of different decomposition techniques, namely EMD, HVD and VMD. After a comprehensive examination, they have concluded that the VMD technique is more suitable for structural monitoring applications than EMD and HVD techniques. A few applications of the EFD technique are already available in the field of structural monitoring, but they are limited to signal features extraction applications [30]. Overall, the available evidence suggests that both VMD and EFD techniques can provide very accurate results. Particularly, their performance depend on the proper setting of the involved control parameters, which should be possibly carried out without any feedback from the analyst in view of automatic applications. The feasibility of the VMD technique for the dynamic identification of the modal parameters of bridge structures has been demonstrated by Yang et al. [14] and Mazzeo et al. [31,32], who also developed suitable strategies towards the automatic optimal tuning of its control parameters. To the authors' knowledge, there is a lack of applications and comparative evaluations related to the modal parameters estimation of real structural systems by means of the EFD technique, which is an impediment towards understanding its accuracy and reliability in automatic dynamic identification. This is the existing gap in the current literature that will be addressed within the present study.

In this paper, an enhanced implementation of the EFD technique is proposed for the automatic dynamic identification of structures from free vibrations. The novel contributions are the following: (i) a smoothing-based improved segmentation of the frequency spectrum; (ii) an iterative automatic process for the optimal tuning of the number of frequency spectrum partitions. The whole identification procedure is completed by implementing an area-based approach for modal damping ratios estimation, whereas a time-domain method based on the phase shift of the free vibration response peaks is employed to identify the mode shapes. The performance of the proposed framework are evaluated through numerical and experimental applications. First, a numerical study based on synthetic signals is performed to quantify objectively the accuracy of the proposed approach. Next, results obtained from two real structures are discussed. The first experimental case-study deals with the dynamic characterization of the cables in a cable-stayed bridge. The second experimental case-study is concerned with the modal identification of a steel railway bridge deck. The critical review and the comparative evaluation of the results obtained by means of the proposed approach demonstrate its correctness and robustness for automatic applications.

2. Automatic modal identification based on the EFD technique

2.1. Modal identification by means of the EFD technique

The proposed identification procedure is based on the detection and extraction of the uni-modal components from the free vibrations of a structural system. This is accomplished by means of the EFD technique, which is an adaptive decomposition method introduced recently by Zhou et al. [24] in order to overcome the limitations typically recognized in the other methods based on Fourier transform such as EWT [22] and FDM [25]. In fact, the EWT performance worsens in case of noisy signals due to an unexpected signal segmentation, which may affect the estimation of the instantaneous frequencies and select trivial components. Similarly, FDM decomposition results have shown to be inconsistent when different frequency scan techniques are adopted to decompose the signal.

The EFD technique allows the decomposition of a multi-modal signal into its uni-modal components and consists of two main steps, namely a spectrum segmentation procedure and the construction of a zero-phase filter bank. The segmentation procedure aims at producing N frequency partitions of the frequency spectrum of the signal to be analyzed whereas the zero-phase filter bank is required to perform the actual decomposition.

The segmentation process is carried out within a normalized frequency domain $[0, \pi]$. Here and henceforth, ω and ν will indicate the circular frequency in [rad/s] and the frequency in [Hz], respectively. Therefore, signal frequency lines must be also normalized. Initially, the

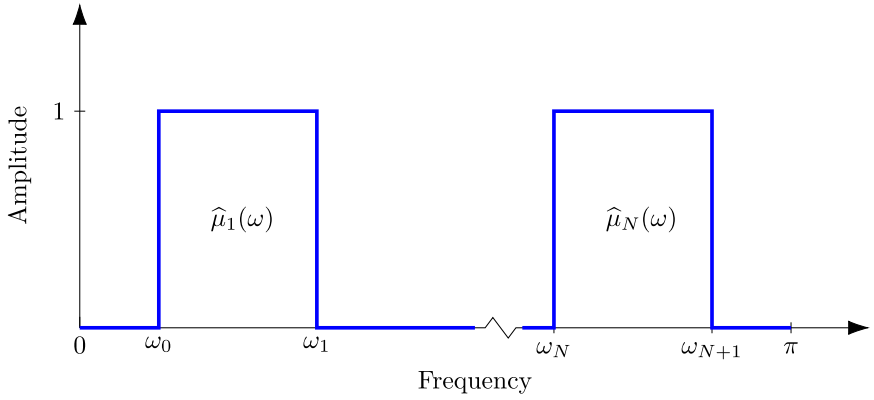

Fig. 1. Zero-phase filter bank used in the EFD technique.

boundaries of the N contiguous frequency partitions, namely $[\omega_{n-1}, \omega_n]$, are detected. Unlike other decomposition techniques that exploit the spectrum segmentation (e.g., EWT), the frequencies ω_0 and ω_N that define the boundary of the first and last frequency partition are not necessarily equal to 0 and π, respectively. Fourier spectrum magnitudes at 0 and π are evaluated through an adaptive process and are sorted together with other local maxima in decreasing order. The first N frequencies corresponding to the largest maximum magnitudes detected in the signal spectrum are sorted in descending order and are denoted as $\{\Omega_1, \ldots, \Omega_N\}$. Furthermore, it is assumed $\Omega_0 = 0$ and $\Omega_{N+1} = \pi$. For each pair of consecutive frequencies Ω_n and Ω_{n+1}, the partition is determined by picking the frequency value ω_n at which a global minimum is attained as follows:

$$\omega_n = \begin{cases} \underset{\omega}{\operatorname{argmin}} \hat{X}_n(\omega) & \text{if } 0 \le n \le N \text{ and } \Omega_n \ne \Omega_{n+1} \\ \Omega_n & \text{if } 0 \le n \le N \text{ and } \Omega_n = \Omega_{n+1}, \end{cases} \tag{1}$$

where $\hat{X}_n(\omega)$ is the Fourier spectrum amplitude between Ω_n and Ω_{n+1} whereas ω is the frequency variable.

The second step of the procedure consists in the construction of a filter bank to perform the decomposition. Zero-phase filters are considered to avoid possible interference due to their transition phases, which can produce mode-mixing effects. The zero-phase filter bank is designed based on the frequency partitions obtained after the segmentation. Hence, the boundary frequencies of each partition identify the cut-off frequencies. Each zero-phase filter is a bandpass filter with no transition phase operating on a given frequency partition $[\omega_{n-1}, \omega_n]$ with unitary amplitude in frequency domain (Fig. 1):

$$\hat{\mu}_n(\omega) = \begin{cases} 1 & \text{if } \omega_{n-1} \le |\omega| \le \omega_n \\ 0 & \text{otherwise.} \end{cases} \tag{2}$$

The zero-phase filter retains most of the Fourier spectrum contribution in the given partition and remaining spectral components out of the cut-off frequency range are eliminated. Let $\hat{f}(\omega)$ be the Fourier transform of the signal to be analyzed, the generic filtered component has the following expression:

$$\hat{f}_n(\omega) = \hat{\mu}(\omega)\hat{f}(\omega) = \begin{cases} \hat{f}(\omega) & \text{if } \omega_{n-1} \le |\omega| \le \omega_n \\ 0 & \text{otherwise} \end{cases} \quad \forall n \in [1, N]. \tag{3}$$

The modal component can be expressed in the time domain by means of the inverse Fourier transform operator $\mathcal{F}^{-1}[\cdot]$ as follows:

$$f_n(t) = \mathcal{F}^{-1}[\hat{f}_n(\omega)] = \int_{-\omega_n}^{-\omega_{n+1}} \hat{f}_n(\omega) e^{j\omega t} d\omega + \int_{\omega_n}^{\omega_{n+1}} \hat{f}_n(\omega) e^{j\omega t} d\omega, \tag{4}$$

where t is the time variable. The reconstructed signal is obtained by simply summing up the extracted components:

$$\tilde{f}(t) = \sum_{n=1}^{N} f_n(t). \tag{5}$$

Central frequencies of all the segments are extracted as the frequency values in the Fourier spectrum at which the first N highest local maxima are attained.

The decomposition of the free vibrations finally allows the identification of all relevant modal parameters of the structure according to the approach described by Mazzeo et al. [31,32]. Particularly, the component central frequencies are taken as modal frequencies of the structural system. Modal damping ratios are obtained by means of an area-based approach that significantly reduces the distortions due to measurement noise as compared to the standard logarithmic decrement method. For the nth modal component, assuming that $2M_n$ areas equal to $S_{m,n}$ each are enclosed between the nth free vibration response function and the time axis, the nth modal damping ratio ξ_n is calculated as follows:

$$\xi_n = \frac{1}{\sqrt{1 + \left(2M_n\pi / R_n\right)^2}}, \tag{6}$$

where R_n is given by:

$$R_n = \ln\left[\frac{\sum_{m=1}^{M_n} S_{m,n}}{\sum_{m=M_n+1}^{2M_n} S_{m,n}}\right]. \tag{7}$$

The value of M_n can be established so as to minimize the uncertainty in modal damping ratio estimation according to Santoshkumar and Khasawneh [33]. Let $v_n^{(s)}(t_p)$ be the local peak value at the time instant t_p corresponding to the nth modal response and the sth measurement point within a sensor network composed of S sensors. The normalized nth mode shape vector can be thus evaluated as follows:

$$\overline{\boldsymbol{\phi}}_n = \left\{ v_n^{(1)}(t_p) \quad v_n^{(2)}(t_p) \quad \ldots v_n^{(s)}(t_p) \quad \ldots v_n^{(S)}(t_p) \right\}^{\top} / \max_{1 \le s \le S} \left| v_n^{(s)}(t_p) \right|. \tag{8}$$

In order to mitigate the possible distortions in the modal shapes identification caused by measurement noise, this operation is repeated by considering multiple local peaks at different time instants and averaging the obtained values.

Although the application of the EFD technique is appealing for modal identification of structures from free vibrations, there are two significant shortcomings that prevent its automatic and robust implementation.

- If the Fourier transform of the signal is noisy, especially close to the peaks, a wrong segmentation is likely to occur. This is due to the fact that trivial peaks not related to modal frequencies occur, which might be wrongly picked up as suitable values of Ω_n. Consequently, trivial local minima points are generated in each frequency partition, thereby misleading the identification of ω_n based on Eq. (1).
- The number of frequency partitions N and, as a consequence, the number of components to be extracted must be assigned before the identification starts. If there is not any a priori information,

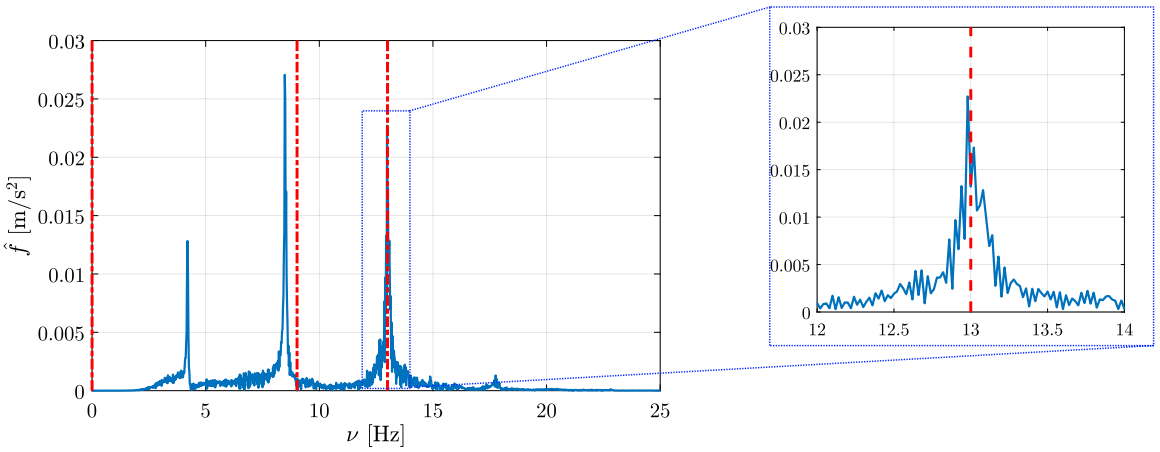

Fig. 2. Incorrect frequency spectrum segmentation of a real signal (dashed vertical lines denote the boundaries of the frequency segments).

then the proper setting of this parameter might be an issue for automatic applications. This, in turn, might jeopardize the correctness of the decomposition procedure.

Efficient strategies are proposed hereafter in order to cope with both these issues.

2.2. Improved segmentation based on smoothed frequency spectrum

Even though the signal might be pre-processed by band-pass filtering to retain only the frequencies falling within the range of interest, the accurate estimation of the frequency spectrum might become challenging due to the residual noise, thereby leading to an incorrect identification of the modal components. This turns out to negatively affect the search for the boundaries of the frequency partitions in the EFD technique according to Eq. (1). In order to figure out the detrimental consequences of this issue, a real signal is considered in Fig. 2 with $N = 3$ (herein, it is considered the experimental cable response of a cable-stayed bridge that will be thoroughly examined later). It is evident in Fig. 2 that the original segmentation process of the signal spectrum wrongly sets a partition boundary at the peak that corresponds to a system frequency ν representative of a vibration mode. As a result, the first two frequency peaks (i.e., the first two vibration modes) are not separated, and mode-mixing occurs. Spectral smoothing approaches have been adopted previously to mitigate the effect of the noise in other decomposition methods and to assist the proper setting of the boundaries of the frequency partitions. Smoothing approaches based on signal spectrum envelope [34,35], moving average filters [36] and Savitzky–Golay filter [37,38] have been adopted in the attempt to improve the spectral representation of the signals.

The proposed solution to improve the segmentation process in the frequency domain for the EFD technique consists in the application of a zero-phase moving average filter in order to smooth the signal spectrum. The moving average filtering operator can be expressed in the following general form:

$$\hat{f}^*[i] = \frac{1}{n^*} \sum_{j=0}^{n^*-1} \hat{f}[i+j], \tag{9}$$

where $\hat{f}[i]$ is the sampled input spectrum, $\hat{f}^*[i]$ is the corresponding sampled output (smoothed spectrum) and n^* is the number of samples used in the moving average. The motivation for using this filter lies in its simplicity of implementation and the minimum number of control parameters. Actually, the only control parameter is the number of samples n^* in the moving average. It is advisable to use a small number of samples n^* in order to avoid too large distortions (i.e., excessive flattening) in the frequency spectrum of the signal. Therefore, the numerical value of this parameter must be related to the frequency resolution adopted for the Fourier transform, which implies that it must depend on the considered number of frequency lines n_{FT} (this latter is usually defined taking into account the recorded signal duration, and it is settled a priori based on the imposed excitation level as well as the expected structural damping). The following rule is thus implemented:

$$n^* = \mathrm{round}[\ln(n_{\mathrm{FT}})/2], \tag{10}$$

where round$[\cdot]$ is the rounding operation to the nearest integer. It must be pointed out that the moving average filter in Eq. (9) produces a delay between original and filtered output such that the higher n^*, the larger the delay. In order to remove the delay between input and output, the zero-phase requirement is invoked in the filter construction (in MATLAB programming language, this result can be obtained by means of the built-in function "filtfilt"). Fig. 3 shows the comparison between the frequency spectrum presented in Fig. 2 and its filtered version obtained by means of Eq. (9): it is evident that the frequency partitions are properly recognized after smoothing, and mode-mixing is now prevented.

It is important to highlight that the construction of the smoothed frequency spectrum only serves at detecting the frequency boundaries for each partition. This means that, once the number of partitions N has been defined, the zero-phase filter bank involved in the EFD technique is applied on the actual frequency spectrum of the signal using the cut-off frequencies recognized from its smoothed frequency spectrum according to Eq. (1).

2.3. Automatic tuning of the number of frequency spectrum partitions

The correct choice of the number of frequency segments N is a critical requisite for the EFD technique because it also defines the number of the extracted uni-modal components. A small value of N will cause mode-mixing (i.e., under-decomposition) whereas a large value will split the contribution of a single mode into several components (i.e., over-decomposition). A rough estimate of this parameter might be obtained by counting the number of peaks in the Fourier transform of the signal. However, if residual noise remains after the filtering process and/or the signal exhibits closely spaced modes, then this criterion becomes too subjective and, ultimately, it is not suitable for automatic applications.

In order to overcome this further limitation of the original EFD technique, an automatic three-steps procedure is here proposed for the optimal tuning of the parameter N. Initially, the Fourier Transform is applied to the considered signal and the resulting frequency spectrum is smoothed by means of the moving average filtering as per Eq. (9), being the filter order defined according to Eq. (10). A few large peaks in the smoothed frequency spectrum will have a physical meaning since they are associated with real modes, whereas the others are small trivial peaks due to the noise. It is evident that the prominence of the

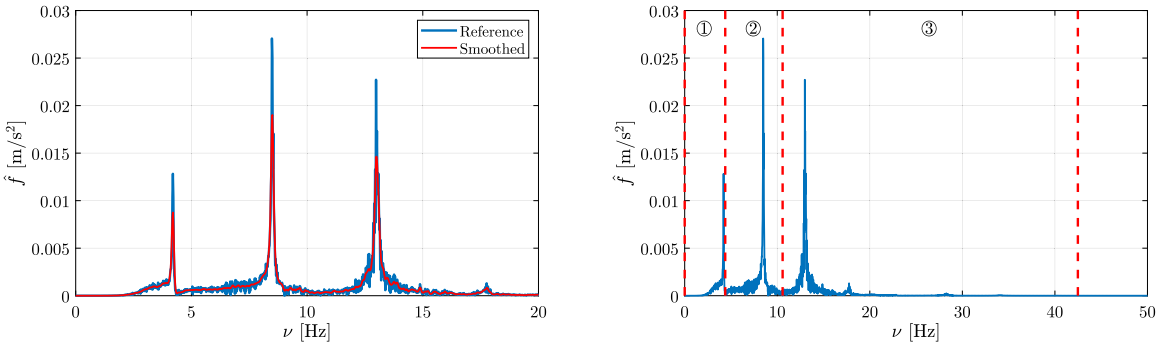

Fig. 3. Smoothing of the signal frequency spectrum: comparison between original and smoothed frequency spectrum (left); correct segmentation of the frequency spectrum after zero-phase moving average filtering (right).

peaks plays a major role in this regard: in fact, only the peaks whose prominence is larger than a given threshold count towards N while they are trivial peaks otherwise. Keeping this in mind, a tentative value of N is initially established in the first step as the number of peaks of the smoothed frequency spectrum whose amplitude $\hat{F}^*$ fulfills the following condition:

$$\hat{F}^* \geq s_1, \tag{11}$$

where s_1 is a threshold parameter. A rational probabilistic criterion is proposed to set the threshold parameter s_1. Let $\hat{F}^*$ be a random variable with non-zero variance $\sigma_{\hat{F}^*}$ and non-zero mean $\mu_{\hat{F}^*}$. Regardless the probabilistic distribution of $\hat{F}^*$, the Chebyshev's inequality [39] states that:

$$\Pr(|\hat{F}^* - \mu_{\hat{F}^*}| \geq k\sigma_{\hat{F}^*}) \leq \frac{1}{k^2}, \tag{12}$$

where $k \in \mathbb{R}$. Since most of the peaks in the frequency spectrum are due to the noise, those corresponding to real modes are in the tail of the probabilistic distribution of $\hat{F}^*$. For a target probability of exceedance equal to 0.90, it follows from Eq. (12) that $s_1 = \mu_{\hat{F}^*} + k\sigma_{\hat{F}^*}$ with $k = 3.162$. It is not recommended to assume a lower target probability of exceedance (i.e., a lower value of k) since this will significantly increase the chance of counting trivial peaks towards N. Conversely, a larger target probability of exceedance (i.e., a larger value of k) will reduce excessively the number of identifiable modes N. It is highlighted, however, that this first step provides a preliminary estimation of N, whose value can be subjected to adjustments in the further steps of the proposed procedure.

The energy lost in the reconstruction process is evaluated in the second step. To this end, a performance reconstruction factor (PRF) is introduced as follows:

$$\mathrm{PRF} = \frac{\left\| f(t) - \sum_{n=1}^{N} f_n(t) \right\|^2}{\|f(t)\|^2}, \tag{13}$$

where $\|\cdot\|$ is a suitable norm operator (e.g., Euclidean norm). This parameter is a measure of the accuracy in the reconstruction of the initial signal through the extracted components. The smaller the PRF is, the closer the reconstructed signal $\tilde{f}(t)$ given by Eq. (5) is to the original one $f(t)$. Having so done, the following condition is checked:

$$\mathrm{PRF} \leq s_2, \tag{14}$$

where s_2 is a threshold parameter. The definition of the threshold parameter s_2 depends on the target fidelity level of the signal reconstruction. A satisfactory trade-off for practical applications is a maximum loss of energy equal to 1%, which implies that $s_2 = 10^{-2}$. If the condition given by Eq. (14) is not fulfilled, this means that the signal is under-decomposed and mode-mixing occurs. Therefore, the number of segments must be at least one unit higher than the final value obtained previously (i.e., it must be assumed $N \mapsto N + 1$).

The last step of the proposed procedure aims at checking whether the obtained value of N produces an over-decomposed signal (i.e., mode-splitting phenomenon occurs). To this end, the signal is decomposed into a number of components equal to N, as it was obtained in the previous step. Hence, the distance between the central frequencies for each couple of consecutive mode functions is evaluated as $\Delta\omega_{n,n+1} = \omega_{n+1} - \omega_n \ \forall n \in [1, N-1]$. Next, it is counted the number of times θ for which the following condition is fulfilled:

$$\Delta\omega_{n,n+1} \leq s_{n,3} \ \forall n \in [1, N-1]. \tag{15}$$

Following such check, the number of frequency partitions is updated as $N \mapsto N - \theta$. The definition of the threshold parameter $s_{n,3}$ is related to the frequency resolution of the EFD technique, that is the minimum distance between two consecutive central frequencies that allows the correct extraction of the corresponding components. Taking into account the available studies [40], it is set as $s_{n,3} = 5\omega_n/100$.

The flowchart in Fig. 4 illustrates the proposed procedure for the automatic tuning of the number of frequency partitions N. Once the optimal value of N is obtained at the end of the procedure detailed in Fig. 4, the cut-off frequencies are recognized from the smoothed frequency spectrum of the signal as per Eq. (1). Finally, the zero-phase filter bank involved in the EFD technique is performed on the actual frequency spectrum of the signal to retrieve the N components.

The proposed procedure for the automatic tuning of N basically looks for its optimal trade-off by preventing both under-decomposition (i.e., mode-mixing) and over-decomposition (i.e., mode-splitting) of the analyzed signal. If the frequency spectrum of the considered signal is smooth enough by itself, then the procedure is likely to converge to the right value of N at the end of the first step whereas the second and the third step holds no influence. This condition, however, is not the most common in practical applications. Consequently, if the frequency spectrum of the signal is rather noisy, then the first step of the procedure will converge to an improper value of N. Unfortunately, the preliminary smoothing of the signal frequency spectrum does not always fix such problem. In order to better clarify the existing issues, a real signal with $N = 3$ is investigated in Fig. 5 (herein, it is considered the experimental cable response of a cable-stayed bridge that will be thoroughly examined later). On the one hand, if the actual signal frequency spectrum is considered, then the high trivial (i.e., non-physical) peaks near the ones corresponding to the real components will lead to an incorrect estimation of the number of frequency segments N. On the other hand, the selection of the value of N from the smoothed frequency spectrum of the signal only can also produce a wrong spectrum segmentation. In fact, since the application of the smoothing technique on the frequency spectrum makes it more flat, the difference between peaks corresponding to trivial and real modes is reduced and both are wrongly counted towards N, thereby overestimating its value and causing the over-decomposition of the signal. By considering the actual frequency spectrum of the signal, the proposed procedure prevents all these issues taking into account simultaneously the peaks prominence

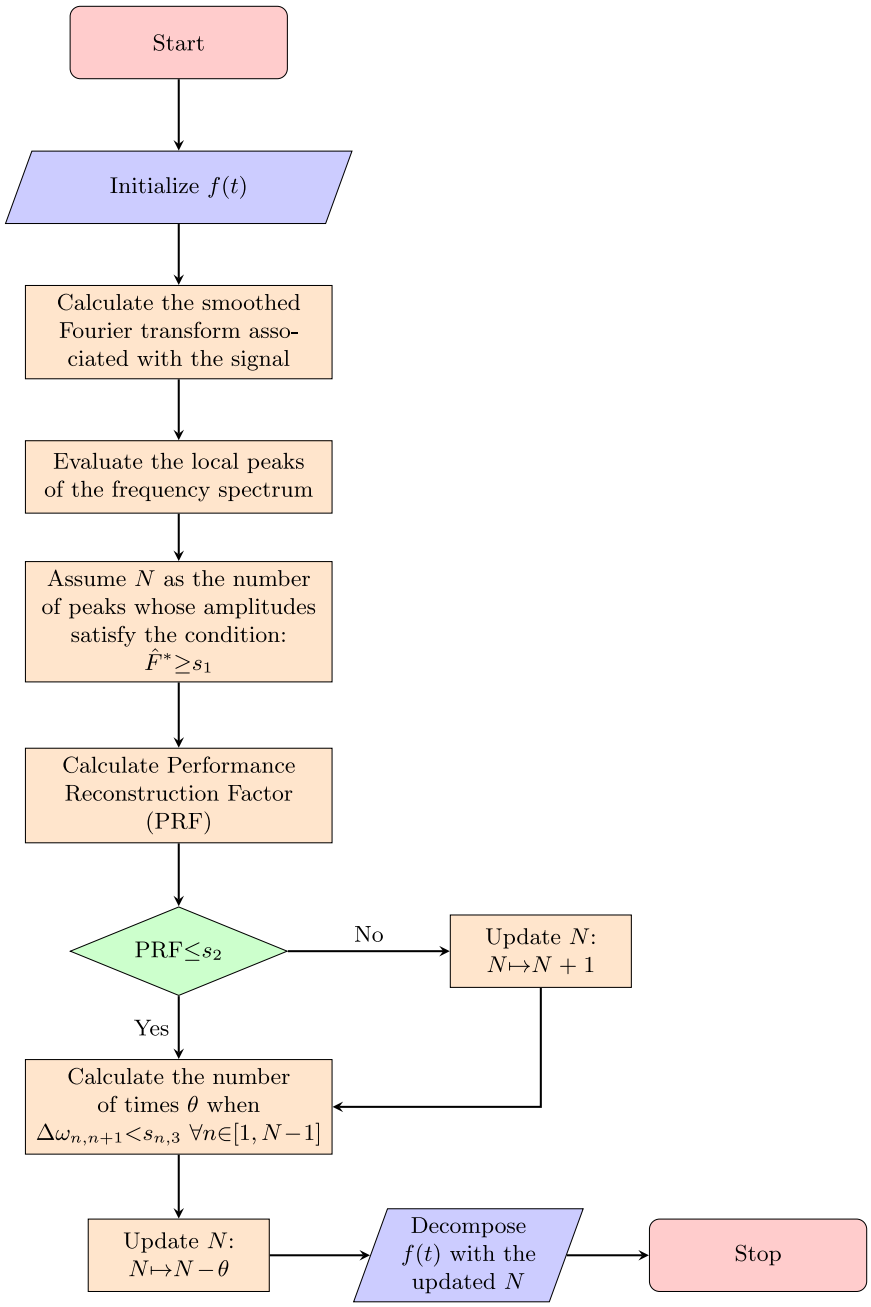

Fig. 4. Flowchart of the proposed automatic selection procedure for the number of the frequency partitions N.

as well as the fidelity of the signal reconstruction and the allowable frequency resolution of the EFD technique. So doing, the number of frequency partitions N and the corresponding boundaries are settled correctly as shown in Fig. 5.

3. Validation on synthetic signals

3.1. Generation of synthetic signals

The proposed improved automatic implementation of the EFD technique is validated against synthetic signals in such a way to quantify objectively its accuracy and robustness. Furthermore, since the reference results are known a priori in case of synthetic signals, the results obtained via the proposed method based on the EFD technique are compared with those carried out by means of the VMD technique [32] in order to assess objectively its performance.

To this end, the typical free vibration response of a multi-degree-of-freedom civil structure is considered, which can be generally expressed as follows:

$$f(t) = \sum_{n=1}^{N} A_n e^{-\xi_n \omega_n t} \cos(\bar{\omega}_n t - \varphi_n) + w(t), \tag{16}$$

where A_n is the nth component amplitude, ξ_n is the nth modal damping ratio, $\omega_n = 2\pi\nu_n$ is the nth modal circular frequency (ν_n being the modal frequency), $\bar{\omega}_n = \omega_n\sqrt{1-\xi_n^2}$ is the corresponding nth circular damped frequency, φ_n is the nth component phase and $w(t)$ is the measurement noise.

Free-noise data are considered to evaluate the accuracy under reference conditions. Noisy data are taken into account in order to test and evaluate the robustness of the identification under more realistic monitoring conditions. The measurement noise $w(t)$ in Eq. (16) is generated as white Gaussian noise with an assigned signal-to-noise ratio

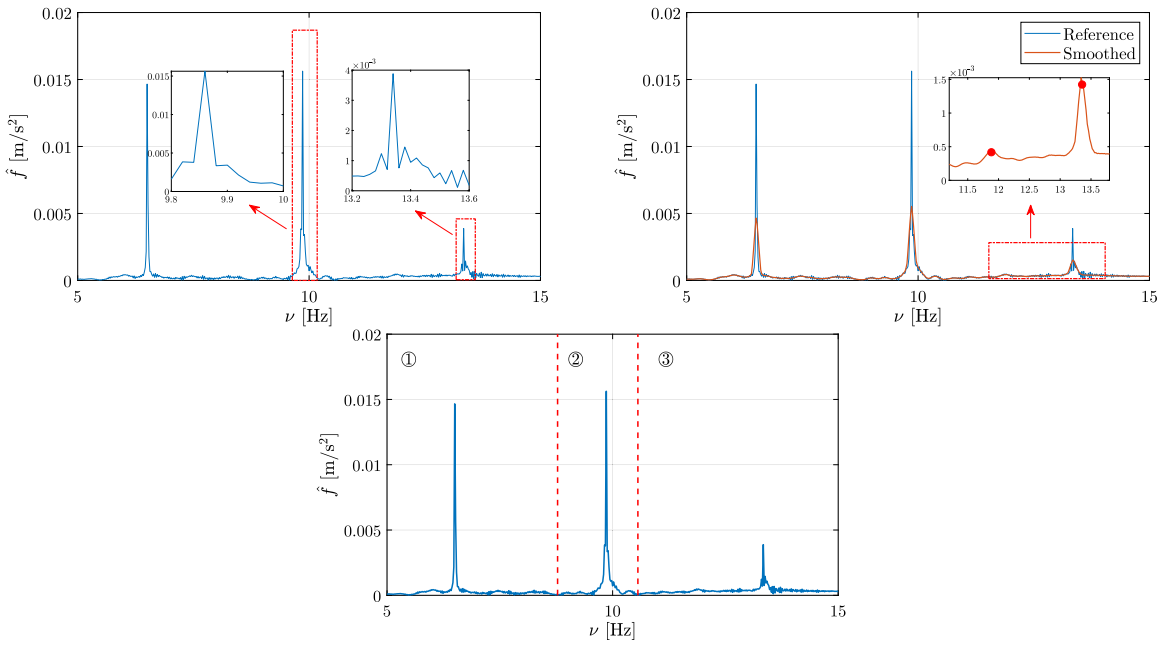

Fig. 5. Possible issues that can jeopardize the correct estimation of the number of the frequency partitions N for a real signal: occurrence of high trivial peaks near the ones corresponding to the real components of the actual frequency spectrum of the signal (top-left); ill-conditioned discrimination between trivial and real peaks (both marked with dots) due to the flattening originated by a preliminary smoothing of the signal frequency spectrum (top-right). Correct spectrum segmentation according to the proposed automatic procedure (bottom).

(SNR), which is defined as follows:

$$\mathrm{SNR} = 10\log_{10}\left(\frac{P_s}{P_n}\right), \tag{17}$$

where P_s and P_n denote the signal and noise average power, respectively. The lower the SNR, the noisier the signal will be. Noisy signals are thus simulated according to the targeted SNR level by assuming an additive-type randomly generated white Gaussian noise $w(t)$ as per Eq. (16). Three noise levels are considered, namely 0 dB, 5 dB and 15 dB (it is pointed out that the resulting synthetic noisy signals are not subjected to preliminary denoising). Because of the inherent randomness of the noise, a set of 100 independent noisy signals is produced for each noise level to allow a statistical appraisal of the final results. It is remarked that modal frequency and damping ratio maintain their nominal value in each noisy signal simulation whereas the randomness is only related to the additive Gaussian white noise $w(t)$, which is fleshly generated for each run.

3.2. Synthetic signal with closely spaced modes

It is considered the free response of a multi-degree-of-freedom system simulated according to Eq. (16) and consisting of four superimposed vibrations modes (i.e., $N = 4$). The natural frequency values are taken equal to $\nu_1 = 1.5$ Hz, $\nu_2 = 3.2$ Hz, $\nu_3 = 3.6$ Hz and $\nu_4 = 10$ Hz. It can be observed that the second and the third natural frequency are rather close to each other (i.e., $\Delta\omega_{2,3}/\omega_3$ about 10%) in order to assess the performance of the proposed approach in detecting closely spaced modes. This condition sometimes occurs when dealing with civil structures, even though it is not very common [41]. The modal damping ratio values are $\xi_1 = 3\%$, $\xi_2 = 1.2\%$, $\xi_3 = 0.8\%$ and $\xi_4 = 2\%$. The amplitudes of the modal components are assumed as $A_1 = 3$, $A_2 = 1.8$, $A_3 = 1.6$ and $A_4 = 5$. All components are in phase (i.e., $\varphi_n = 0\ \forall n$) and a sampling frequency $F_s = 1$ kHz is adopted.

To begin with, the case of a free-noise signal is analyzed and thus the measurement noise $w(t)$ in Eq. (16) is initially null. Fig. 6 shows the considered signal and the corresponding frequency spectrum.

It can be inferred from Fig. 6 that the proposed algorithm for the selection of N (see Fig. 4) enables the extraction of the right number of frequency partitions through the EMD technique. Taking into account the Nyquist–Shannon sampling theorem, the following frequency boundaries are obtained: $\nu_A = 0$, $\nu_B = 2.5$ Hz, $\nu_C = 3.4$ Hz, $\nu_D = 7.7$ Hz and $\nu_E = 499.9$ Hz. Fig. 7 shows that there exist an almost perfect match between the automatically extracted components of the considered free-noise synthetic signal and the corresponding reference analytical modes.

The same free-noise synthetic signal is now decomposed by means of the VMD technique. To this end, some control parameters must be set in advance to perform the decomposition [27]. Particularly, two key control parameters govern the performance of the VMD technique, namely the number of expected modes K and the quadratic penalty factor α [19,42]. The control parameter K defines the number of uni-modal components to be extracted from the signal. Once again, therefore, an over-decomposition of the signal is obtained for a high value of K while a low value of K can produce mode-mixing effects. The control parameter α rules the amplitude of the bandwidth. If α is small, then the bandwidths will be overestimated and closely spaced modes might be grouped by causing mode-mixing effects. Conversely, a too high value of α can produce distortions that will compromise the fidelity of the signal reconstruction. The main advantage of the EFD technique over the VMD technique is thus related to the lower number of control parameters to be tuned: while N only must be determined within the EFD technique, K and α must be defined to perform the VMD technique. It must be also remarked that, even if the correct value of K is singled out, the results of the VMD technique are very sensitive to variations of the value of α. Additionally, in view of automatic applications, the proper selection of the parameter N in the EFD technique by means of the proposed procedure is rather straightforward as compared to the optimal tuning of the parameters K and α involved in the VMD technique. In this regard, the optimal tuning of K in the VMD technique according to the procedure proposed by Mazzeo et al. [32] needs the calculation of a stabilization diagram based on the concept of minimum correlation between mode functions. Such a stabilization diagram then provides a feasible set of values for α, from which the optimum is determined taking into account the power spectrum of the processed signal and each mode function extracted iteratively by means of the VMD technique. More details about the

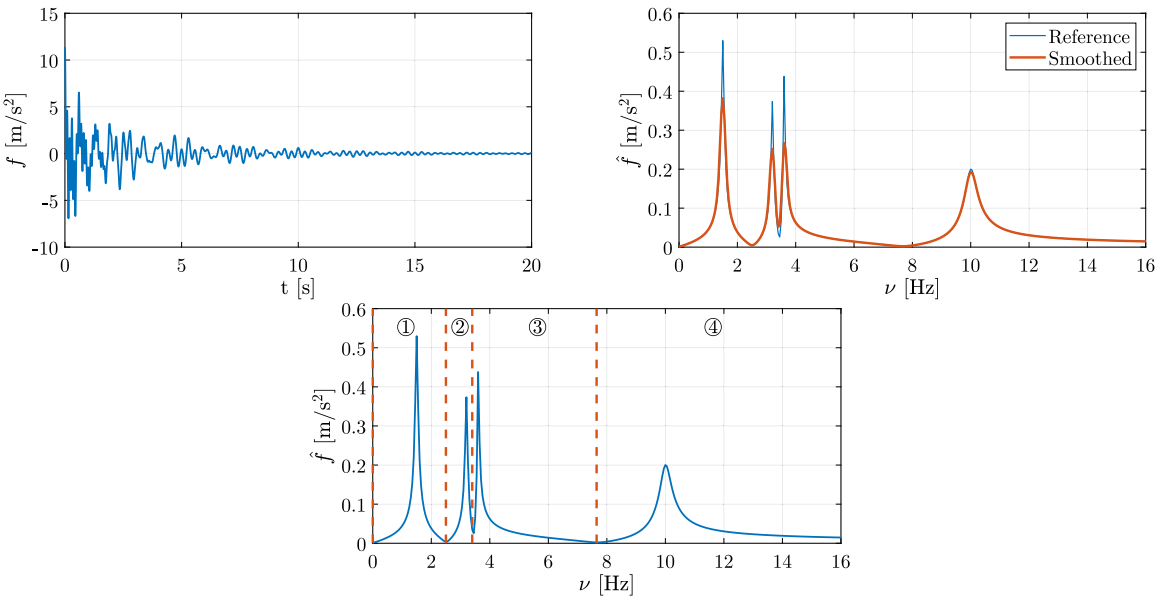

Fig. 6. Synthetic free vibration response with closely spaced modes: free-noise synthetic signal (top-left); comparison between original and smoothed frequency spectrum of the signal (top-right); frequency spectrum segmentation by means of the proposed automatic implementation of the EFD technique (bottom).

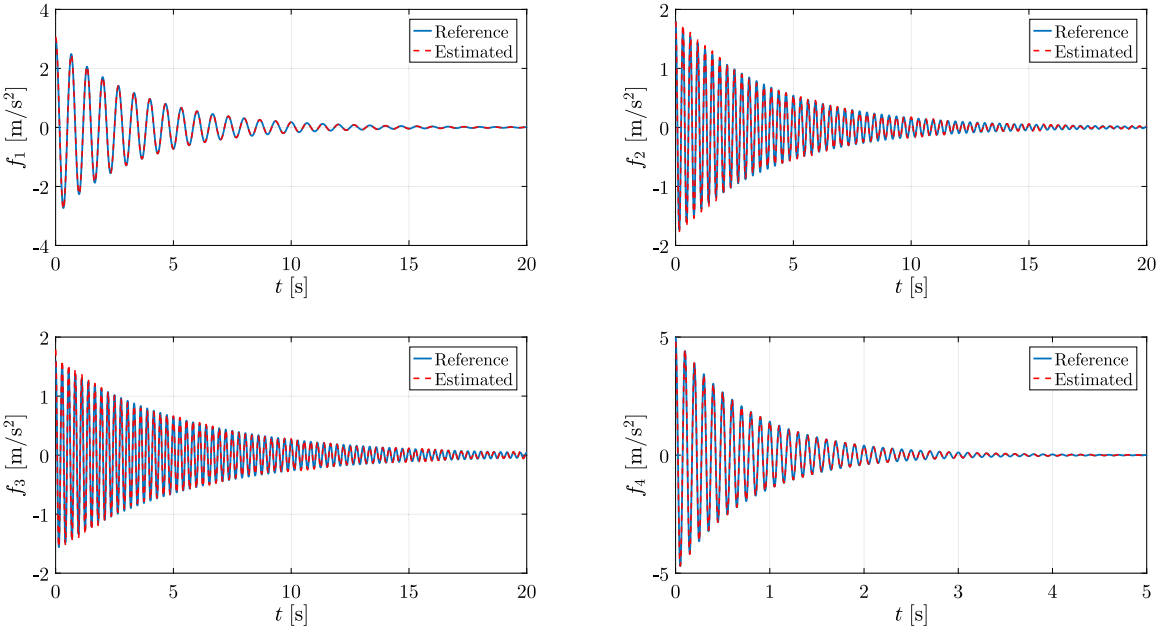

Fig. 7. Synthetic free vibration response with closely spaced modes: comparison between the reference analytical modes and the components extracted using free-noise data by means of the proposed automatic implementation of the EFD technique.

automatic optimal tuning procedure for the control parameters of the VMD technique are provided by Mazzeo et al. [32].

Fig. 8 illustrates the results carried out by applying the VMD technique. The decomposition is initially performed by assuming $K = 4$ and the default value $\alpha = 10^3$. Lastly, the automatic tuning procedure presented by Mazzeo et al. [32] is applied, which provides $K = 4$ and $\alpha = 5.7 \cdot 10^5$. The comparison between the extracted components and the corresponding reference analytical modes demonstrate the correctness of the VMD technique, provided that the numerical values of both K and α are properly selected.

Tables 1–2 provide the results obtained by implementing the VMD technique with default value of α (i.e., $\alpha = 10^3$, given $K = 4$) and the optimal value of the control parameters estimated according to Mazzeo et al. [32] (i.e., $\alpha = 5.7 \cdot 10^5, K = 4$). The results obtained by means of the proposed implementation of the EFD technique are also reported.

The analysis of the results listed in Table 1 demonstrates that the VMD technique as well as the EFD technique are able to identify accurately the natural frequencies of the considered free-noise synthetic signal when they are properly implemented. The exact value of the natural frequencies is retrieved by applying the EFD technique. A negligible error is obtained by estimating the natural frequencies through the VMD technique, provided that the value of α is properly optimized (very large errors can occur for lower modes otherwise). Remarkably, Table 2 also demonstrates that the way by which the signal is decomposed has significant effects on the accuracy of the modal damping ratio identification, even through noiseless data are considered. As regards

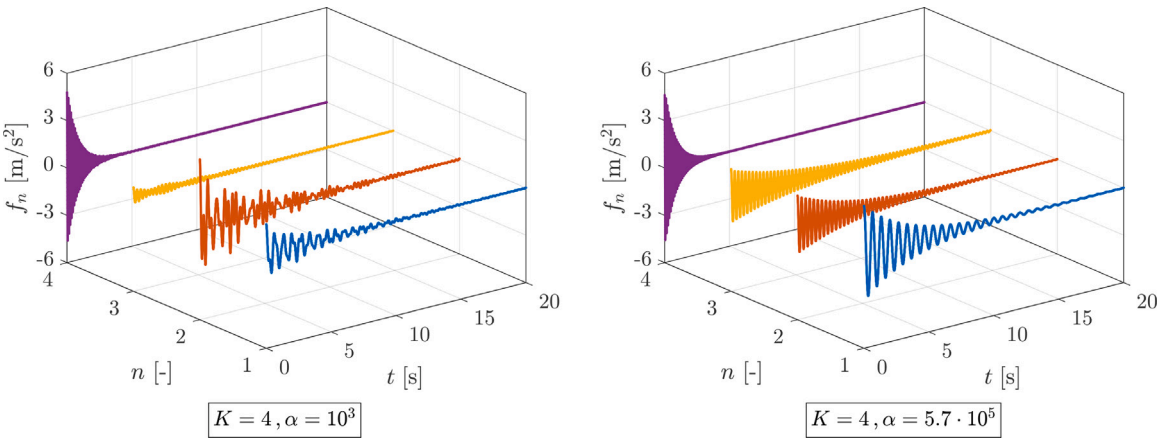

Fig. 8. Synthetic free vibration response with closely spaced modes: modal components extracted by means of the VMD technique using free-noise data for the default value $\alpha = 10^3$ (left) and $\alpha = 5.7 \cdot 10^5$ as estimated automatically according to Mazzeo et al. [32] (right).

Table 1
Synthetic free vibration response with closely spaced modes: identification of the natural frequencies using free-noise data by applying the VMD technique (with both default and optimal values of α and K) and the EFD technique (with N calculated automatically according to the proposed procedure).

Mode	VMD (default α)		VMD ($\alpha = 5.7 \cdot 10^5$)		EFD (proposed)	
	Estimated frequency [Hz]	Relative error [%]	Estimated frequency [Hz]	Relative error [%]	Estimated frequency [Hz]	Relative error [%]
1	1.76	17.33	1.4988	0.08	1.5	0
2	2.54	20.63	3.1988	0.04	3.2	0
3	3.57	0.83	3.5993	0.02	3.6	0
4	9.98	0.20	9.9882	0.12	10	0

Table 2
Synthetic free vibration response with closely spaced modes: identification of the modal damping ratios using free-noise data by applying the VMD technique (with both default and optimal values of α and K) and the EFD technique (with N calculated automatically according to the proposed procedure).

Mode	VMD (default α)		VMD ($\alpha = 5.7 \cdot 10^5$)		EFD (proposed)	
	Estimated damping [%]	Relative error [%]	Estimated damping [%]	Relative error [%]	Estimated damping [%]	Relative error [%]
1	3.4	13.33	3	0	3	0
2	1.7	41.67	1.19	0.83	1.21	0.83
3	0.43	46.25	0.86	7.5	0.8	0
4	2	0	1.98	1	2	0

the application of the VMD technique, average and maximum value of the relative error in modal damping ratios identification are equal to 2.33% and 7.5%, respectively, after a suitable calibration of α (unacceptable errors are obtained otherwise). Average and maximum value of the relative error in modal damping ratios identification are equal to 0.20% and 0.83% when the EFD technique is applied. The maximum error in modal damping ratio identification is achieved when closely spaced signal components are processed, regardless the way by which the free-noise signal is decomposed. Hence, although the identification of the modal damping ratios from free-noise data via VMD technique is still very good, the corresponding average and maximum value of the relative error are about ten times those obtained by applying the EFD, which thus results more accurate.

The robustness against the noise of the identification is now assessed. Fig. 9 shows some sample noisy signals generated according to different noise levels as well as the frequency spectrum corresponding to the sample noisy signal with highest noise level. Fig. 9 confirms the feasibility of the proposed procedure (see Fig. 4) for the automatic definition of the N components to be extracted by means of the EFD technique even in case of noisy data. It is noted that the segmentation procedure detects and removes most of the noise from the partitions in the high-frequency region of the signal spectrum. The comparison between Fig. 9 and Fig. 6 highlights that the segmentation process reduces the width of the last partition.

It has been found that the identification of the natural frequencies is not influenced significantly by the decomposition technique even in case of external disturbances. Therefore, natural frequencies can be properly identified from noisy data for all values of the SNR by using either the VMD technique or the EFD technique. The estimation of the modal damping ratio is instead more sensitive to the measurement noise, as it emerges from the results listed into Tables 3–4.

The results in Table 3 demonstrate that the application of the EFD technique based on the proposed automatic segmentation of the signal spectrum provides very good estimates of the modal damping ratios even in case of noisy signals. As expected, the larger is the noise level, the larger is the error. This confirms that the proposed automatic implementation of the EFD technique provides a very good and robust frequency spectrum decomposition for modal damping ratio identification. Once again, the accuracy of the automatic procedure based on the VMD technique proposed by Mazzeo et al. [32] is satisfactory, but slightly larger errors are found. In fact, the highest average and maximum value of the relative errors in damping ratios identification by means of the EFD technique are equal to 5.80% and 38.40%, respectively, for the highest noise level. The corresponding values of the relative errors obtained via the VMD technique are 6.25% and 40.01%, respectively.

The use of the area-based approach for modal damping ratios as proposed in the present study also plays an important role in this regard.

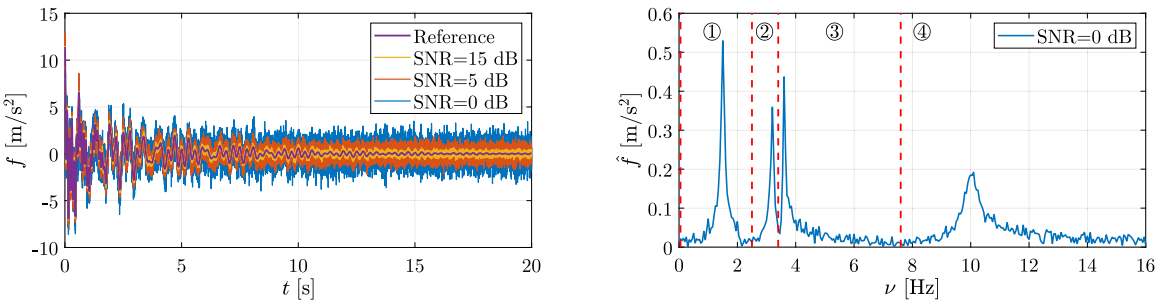

Fig. 9. Synthetic free vibration acceleration response with closely spaced modes: noisy synthetic signals for different values of the SNR (left); frequency spectrum segmentation of the synthetic signal with the highest noise level by means of the proposed automatic implementation of the EFD technique (right).

Table 3
Synthetic free vibration response with closely spaced modes: identification of the modal damping ratios using noisy data by applying the EFD technique (with N calculated automatically according to the proposed procedure). Average value and standard deviation of the estimated modal damping ratio are reported. Moreover, mean and maximum value (within brackets) of the relative error are provided.

Mode	SNR = 15 dB			SNR = 5 dB			SNR = 0 dB		
	Estimated damping [%]	Standard deviation [–]	Relative error [%]	Estimated damping [%]	Standard deviation [–]	Relative error [%]	Estimated damping [%]	Standard deviation [–]	Relative error [%]
1	2.99	1.96E−2	0.08 (2.11)	2.98	6.08E−2	0.50 (6.51)	2.97	1.22E−1	0.77 (9.37)
2	1.21	1.17E−2	0.56 (3.82)	1.22	3.81E−2	1.56 (10.21)	1.24	6.83E−2	3.15 (15.77)
3	0.82	9.36E−3	2.55 (5.67)	0.84	3.13E−2	4.89 (15.08)	0.85	5.78E−2	5.80 (23.45)
4	2.01	1.89E−2	0.50 (3.10)	2.04	3.34E−1	2.21 (17.66)	1.94	4.59E−1	3.00 (38.40)

Table 4
Synthetic free vibration response with closely spaced modes: identification of the modal damping ratios using noisy data by applying the VMD technique (with α and K calculated automatically according to the procedure proposed by Mazzeo et al. [32]). Average value and standard deviation of the estimated modal damping ratio are reported. Moreover, mean and maximum value (within brackets) of the relative error are provided.

Mode	SNR = 15 dB			SNR = 5 dB			SNR = 0 dB		
	Estimated damping [%]	Standard deviation [–]	Relative error [%]	Estimated damping [%]	Standard deviation [–]	Relative error [%]	Estimated damping [%]	Standard deviation [–]	Relative error [%]
1	2.99	2.20E−2	0.33 (2.20)	2.98	8.31E−2	0.60 (9.26)	2.93	1.51E−1	2.33 (15.88)
2	1.17	2.13E−2	2.41 (6.61)	1.16	6.74E−2	2.50 (15.78)	1.15	1.46E−1	4.17 (35.02)
3	0.85	1.32E−2	6.29 (9.49)	0.84	4.18E−2	5.59 (15.66)	0.75	7.42E−2	6.25 (21.99)
4	1.95	2.58E−2	2.79 (6.33)	1.94	8.17E−2	2.86 (14.01)	1.93	4.70E−1	3.50 (40.01)

In fact, if the standard logarithmic decrement method is applied after signal decomposition as proposed by He et al. [43], then the accuracy of the modal damping ratios identification reduces significantly. It can be noted in Table 5 that, if the EFD technique is employed in combination with the standard decrement logarithmic method to identify the relevant modes, then the highest relative error for the highest noise level is about 12.93% whereas the maximum relative error is 81.28%. This confirms that the EFD technique should be implemented together with a suitable modal damping ratio identification procedure in order to obtain the best estimates of the modal characteristics of the structures.

3.3. Synthetic signal with minor mode

It is now considered the free response of a multi-degree-of-freedom system simulated according to Eq. (16) and consisting of three superimposed vibrations modes (i.e., $N = 3$). The natural frequencies are equal to $\nu_1 = 1.5$ Hz, $\nu_2 = 3.5$ Hz and $\nu_3 = 7$ Hz whereas modal damping ratios are equal to $\xi_1 = 3\%$, $\xi_2 = 5\%$, $\xi_3 = 3\%$. The amplitudes of the three signal components are equal to $A_1 = 1.5$, $A_2 = 0.95$ and $A_3 = 4$. All components are in phase (i.e., $\varphi_n = 0$ $\forall n$). Different noise levels are considered, and a sampling frequency $F_s = 1$ kHz is adopted. Fig. 10 shows some sample noisy signals generated according to different noise levels as well as the frequency spectrum corresponding to the sample noisy signal with the highest noise level. The dynamic identification in case of a minor vibration mode is the main issue that the present benchmark aims at dealing with. In fact, it is evident from the frequency spectrum in Fig. 10 that the peak corresponding to the second mode is much lower than the peaks related to the first and third mode. This condition can occur when the free vibrations are due to a force or displacement applied close to a nodal point of a highly damped vibration mode. As a consequence, such vibration mode is lowly excited and its accurate identification can be challenging.

Once again, natural frequencies are well identified by means of either the EFD technique or the VMD technique. The performances of the two approaches diverge significantly when the modal damping ratios identification is examined, as it can be observed by comparing the results listed in Tables 6–7.

On average, Tables 6–7 demonstrate that the implemented identification approaches based on the EFD technique and the VMD technique

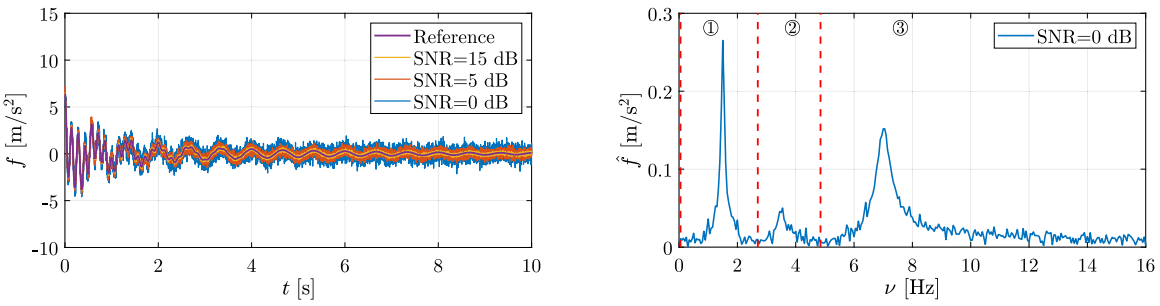

Fig. 10. Synthetic free vibration acceleration response with minor mode: noisy synthetic signals for different values of the SNR (left); frequency spectrum segmentation of the synthetic signal with the highest noise level by means of the proposed automatic implementation of the EFD technique (right).

Table 5
Synthetic free vibration response with closely spaced modes: identification of the modal damping ratios using noisy data by applying the EFD technique (with N calculated automatically according to the proposed procedure) in combination with the standard decrement logarithmic method. Average value and standard deviation of the estimated modal damping ratio are reported. Moreover, mean and maximum value (within brackets) of the relative error are provided.

Mode	SNR = 15 dB			SNR = 5 dB			SNR = 0 dB		
	Estimated damping [%]	Standard deviation [–]	Relative error [%]	Estimated damping [%]	Standard deviation [–]	Relative error [%]	Estimated damping [%]	Standard deviation [–]	Relative error [%]
1	2.94	4.71E−2	1.85 (5.87)	2.96	1.50E−1	1.16 (13.63)	3.14	2.73E−1	4.66 (22.55)
2	1.33	1.81E−2	11.05 (15.00)	1.32	5.81E−2	10.35 (23.77)	1.33	1.07E−1	10.71 (47.53)
3	0.89	3.47E−2	11.49 (21.72)	0.88	1.04E−1	10.05 (43.98)	0.90	2.26E−1	12.93 (81.28)
4	2.05	3.38E−2	2.25 (5.77)	2.11	2.78E−1	5.29 (18.13)	2.16	9.58E−1	8.18 (57.94)

Table 6
Synthetic free vibration response with minor mode: identification of the modal damping ratios using noisy data by applying the EFD technique (with N calculated automatically according to the proposed procedure). Average value and standard deviation of the estimated modal damping ratio are reported. Moreover, mean and maximum value (within brackets) of the relative error are provided.

Mode	SNR = 15 dB			SNR = 5 dB			SNR = 0 dB		
	Estimated damping [%]	Standard deviation [–]	Relative error [%]	Estimated damping [%]	Standard deviation [–]	Relative error [%]	Estimated damping [%]	Standard deviation [–]	Relative error [%]
1	2.99	2.27E−2	0.03 (1.86)	2.98	7.15E−2	0.31 (5.55)	2.97	1.25E−1	0.81 (9.64)
2	5.03	1.08E−1	0.59 (6.38)	5.09	3.09E−1	1.77 (14.17)	4.90	5.41E−1	1.99 (25.10)
3	3.00	1.78E−2	0.08 (1.44)	3.01	5.08E−2	0.36 (4.48)	2.98	9.37E−2	0.55 (7.92)

Table 7
Synthetic free vibration response with minor mode: identification of the modal damping ratios using noisy data by applying the VMD technique (with α and K calculated automatically according to the procedure proposed by Mazzeo et al. [32]). Average value and standard deviation of the estimated modal damping ratio are reported. Moreover, mean and maximum value (within brackets) of the relative error are provided.

Mode	SNR = 15 dB			SNR = 5 dB			SNR = 0 dB		
	Estimated damping [%]	Standard deviation [–]	Relative error [%]	Estimated damping [%]	Standard deviation [–]	Relative error [%]	Estimated damping [%]	Standard deviation [–]	Relative error [%]
1	2.99	3.05E−2	0.08 (3.24)	2.94	1.07E−1	1.95 (12.60)	2.89	2.04E−1	3.63 (17.80)
2	5.10	9.40E−2	1.94 (16.14)	4.83	8.54E−1	3.46 (47.39)	4.43	12.49E−1	11.47 (54.04)
3	2.97	1.84E−2	0.89 (12.38)	2.84	4.51E−1	5.36 (53.83)	2.55	6.89E−1	14.92 (55.75)

exhibit almost similar performance in terms of modal damping ratio identification for a low noise level. The accuracy of the VMD technique is still satisfactory on average for mid-high noise levels, but a significant degradation is evident with respect to the EFD technique. In fact, the largest value of the average relative error is less than 2% for both signal decomposition techniques at SNR = 15 dB, but it is almost equal 15% for SNR = 0 dB if the modal damping ratios are obtained through the VMD technique while is still less than 2% if the EFD technique is employed instead. The critical analysis of the results in Tables 6–7 especially highlights the different robustness between the two approaches. Standard deviations of the modal damping ratios estimated according to the proposed automatic implementation of the EFD technique are lower than the corresponding values obtained through the VMD technique. Furthermore, a deeper inspection of the maximum

Fig. 11. Overview of stay-cabled bridge over the Garigliano river investigated in the present work.

relative errors demonstrates that the VMD technique sometimes fails to provide satisfactory estimates of the modal damping ratios (i.e., a relative error larger than 25% occurred for the second and the third modal damping ratio in 1%, 5% and 18% of the simulations at SNR = 15 dB, SNR = 5 dB and SNR = 0 dB, respectively). Conversely, the automatic implementation of the EFD technique presented in the current study dramatically reduces the number of failed identifications and is really effective in alleviating the maximum value of the relative error, thereby ensuring a more consistent estimation of the modal damping ratios than the VMD technique. The identification of the minor mode is especially challenging for both signal decomposition techniques. It can be deduced from Table 7 that the inaccurate identification of the minor mode can affect, to a large extent, the reliable identification of higher modes if the VMD technique is employed. Indeed, it can be inferred from Table 7 that the identification of the vibration mode following the minor mode is less accurate than the first vibration mode when the VMD technique is adopted. Conversely, it is noteworthy to observe that the proposed implementation of the EFD technique prevents the propagation of the larger errors associated with the identification of the minor mode. This is deduced from the results in Table 6, which show that the first and the third modal damping ratios are identified with a similar accuracy level when the EFD technique is adopted.

4. Experimental application on a roadway bridge

The first experimental application deals with a roadway bridge. The bridge over the Garigliano river (Italy) is here examined, which is a cable-stayed structure completed in 1993 as part of the highway network that connects Rome and Naples (Fig. 11). The bridge is made up of two 90 m long spans, which are simply supported at one end and framed to the central pylon at the other end. The precast prestressed concrete box girders are sustained by 9 couples of cables per span with variable length ranging from 23 m to 87.5 m. The cables are connected at different elevations to a central pylon with variable cross-section and whose height is 30 m with respect to the bridge deck level.

The experimental dynamic assessment of deck and cables was already performed in previous studies by exploiting the ambient excitation [44,45]. Another monitoring campaign has been designed to further check the cables' condition. To this end, free vibration tests were performed in order to optimize both cost and time of the monitoring campaign. The dynamic response has been monitored by means of a couple of uniaxial accelerometers with sensitivity equal to 10 V/g, which were mounted on the two faces of a steel angular element in such a way to record both vertical and horizontal accelerations with respect to the longitudinal axis of each cable. This angular element equipped with two accelerometers has been fixed to the bridge cable at an average height equal to 3.8 m by means of nylon straps (Fig. 12). The excitation on the cables was induced by applying an impulsive load along two distinct directions (i.e., longitudinal and transversal direction with respect to the longitudinal axis of the cables). The acceleration response has been recorded with a sampling frequency equal to F_s = 200 Hz. In this study, only the signals recorded on the west side of the bridge (for both traffic directions) are analyzed.

Natural frequencies and damping ratios have been identified from the free vibration response of each cable by means of the EFD technique assisted by the proposed procedure for the optimal automatic tuning of the control parameter N.

As an example, Fig. 13 shows the free vibration response of the shortest bridge cable (Rome direction) due to a vertical impulse load and the corresponding frequency spectrum. The proposed procedure illustrated in Fig. 4 provides the correct value of N for the analyzed signal, as it is shown in Fig. 14. A total of $N = 4$ frequency partitions has been identified and the corresponding extracted modes are plotted into Fig. 15. For the considered signal, the estimated natural frequencies are $\nu_1 = 6.42$ Hz, $\nu_2 = 13.16$ Hz, $\nu_3 = 20.52$ Hz, and $\nu_4 = 28.52$ Hz, while the modal damping ratios are equal to $\xi_1 = 0.12\%$, $\xi_2 = 0.16\%$, $\xi_3 = 0.22\%$, $\xi_4 = 0.29\%$.

The proposed identification procedure has been applied automatically (i.e., without any external feedback) to all the available experimental data. For both roadway directions, four recordings were obtained for each cable depending on the orientation of the sensor and the specific direction of the applied impulsive excitation (for a total of 72 signals). On the one hand, missing results for a cable are due to the fact that the corresponding recording file was corrupted. On the other hand, the unsuccessful identification of the highest mode in a few cables is attributable to the fact that the magnitude of the corresponding response was not large enough to allow its identification. The identified modal frequencies for the first four modes of the bridge cables are listed in Table 8 (natural frequency values are averaged over all the available signals for the examined cable). It can be observed in Table 8 that the natural frequencies of the higher modes are approximately integer multiples of the fundamental frequency, in agreement with classical theoretical results about the cable dynamics. These results are also in agreement with previous studies that have exploited ambient vibrations [44,45].

The natural frequencies of the cables have been also calculated numerically in order to evaluate the general correctness of the experimental estimates obtained by means of the proposed identification procedure. Therefore, the following relationship proposed by Fang et al. [46] is considered to evaluate the natural frequencies of the cables from the tensile force:

$$T = 4\pi^2 m l^2 \frac{\nu_n}{\gamma_n} - \frac{EI}{l^2}\gamma_n^2, \tag{18}$$

where m is the density of the cable, l is its length, EI is the flexural stiffness of the cable, n is the mode number, $\gamma_n = n\pi + A\psi_n + B\psi_n^2$ with

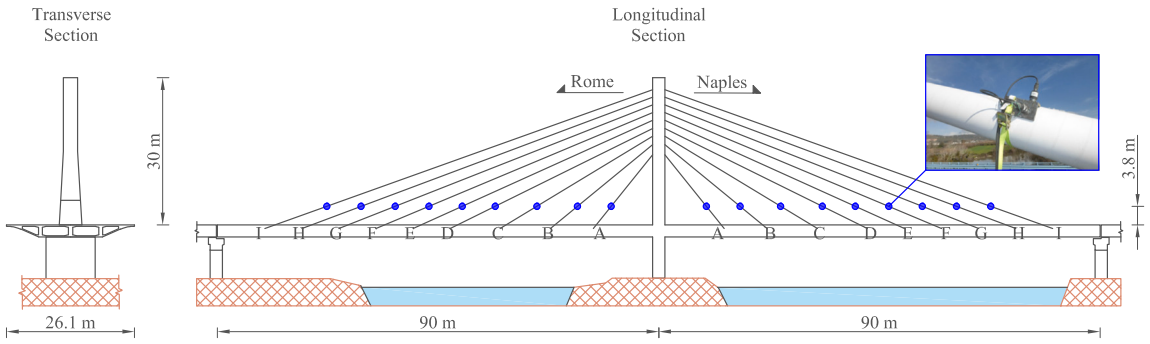

Fig. 12. Layout of the stay-cabled bridge over the Garigliano river and details about the sensors position for monitoring the dynamic response of the cables.

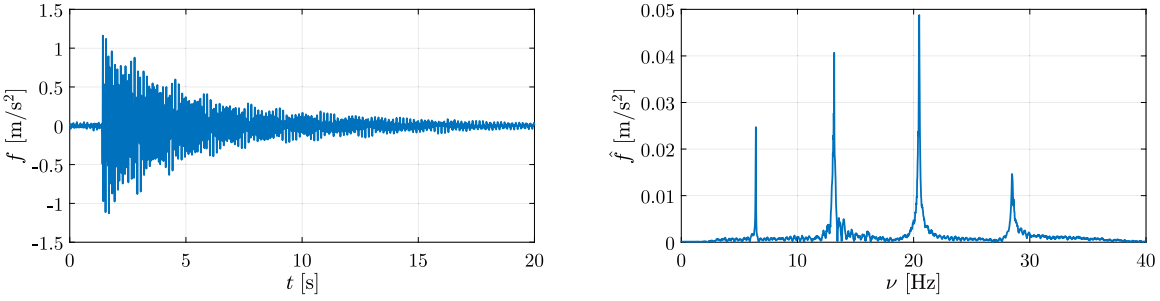

Fig. 13. Dynamic response of the shortest bridge cable (Rome direction): free vibration acceleration signal due to a vertical impulse load (left); frequency spectrum of the considered signal (right).

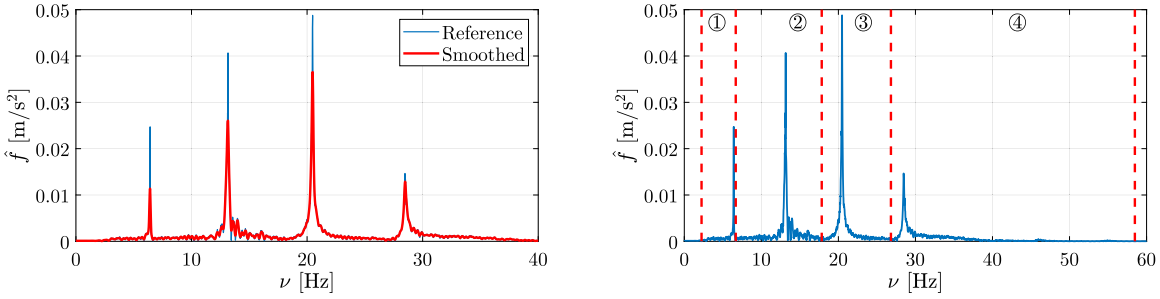

Fig. 14. Dynamic response of the shortest bridge cable (Rome direction): comparison between original and smoothed frequency spectrum of the considered signal (left); frequency spectrum segmentation of the considered signal (right).

Table 8
Natural frequencies for the first four vibration modes of the bridge cables estimated by means of the proposed procedure based on the EFD technique.

Cable	Rome direction				Naples direction			
	ν_1 [Hz]	ν_2 [Hz]	ν_3 [Hz]	ν_4 [Hz]	ν_1 [Hz]	ν_2 [Hz]	ν_3 [Hz]	ν_4 [Hz]
A	6.41	13.14	20.48	28.54	6.13	12.57	19.60	–
B	4.21	8.52	13.04	–	4.19	8.48	13.00	17.81
C	3.23	6.51	9.88	13.38	3.21	6.48	9.83	13.32
D	–	–	–	–	2.53	5.06	7.66	10.33
E	2.16	4.34	6.55	8.79	2.16	4.34	6.54	8.78
F	1.87	3.76	5.68	7.61	1.90	3.80	5.72	7.69
G	1.65	3.32	5.00	6.70	1.67	3.37	5.05	6.77
H	1.50	3.00	4.51	6.03	1.49	2.99	4.50	6.02
I	1.26	2.51	3.78	5.06	1.28	2.54	3.83	5.14

$\psi_n = \sqrt{EI/m\omega_n^2 l^4}$, $A = -18.9 + 26.2n + 15.1n^2$ and $B = 290$ for $n = 1$, 0 otherwise. The elastic modulus E for harmonic steel was assumed equal to 198,000 MPa, while the moment of inertia I ranges between 0.015 m^4 and 0.019 m^4 depending on the specific cross-section of each cable. The cable tensile force T in Eq. (18) is determined according to the original design and includes possible variations due to traffic loads and thermal gradients. Moreover, the actual tensile force of the cables is properly reduced (as compared to the initial value) to also account for tension losses due to steel relaxation according to Eurocode 2 [47]. Relaxation losses are calculated using the following expression:

$$\frac{\Delta\sigma_{pr}}{\sigma_{pi}} = 5.39\rho_{1000}e^{6.7\eta}\left(\frac{\tau}{1000}\right)^{0.75(1-\eta)}10^{-5}, \tag{19}$$

where σ_{pi} is the initial prestress level, $\Delta\sigma_{pr}$ is the tensile loss due to relaxation, τ is the time elapsed after tensioning, $\eta = \sigma_{pi}/f_{pk}$ is the initial prestress level normalized with respect to the characteristic

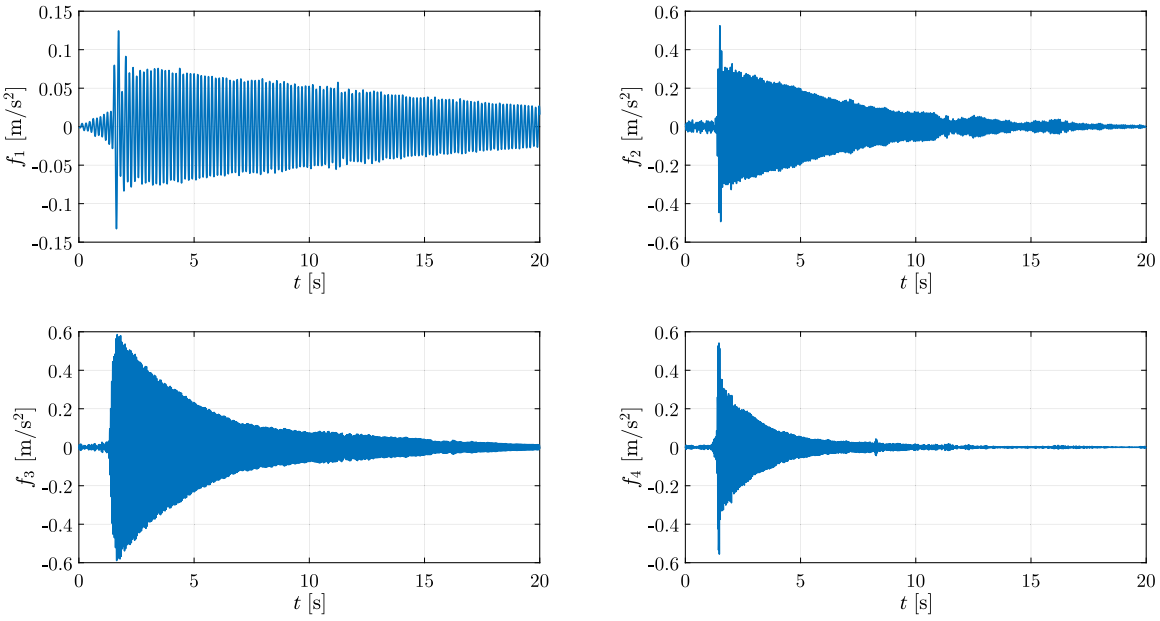

Fig. 15. Dynamic response of the shortest bridge cable (Rome direction): components extracted from the considered acceleration signal via EFD technique.

value of tensile strength of the prestressing steel and $\rho_{1000} = 8$ is the relaxation loss at 1000 h after tensioning for ordinary tendons at a mean temperature equal to 20 °C. In this study, it is assumed $f_{pk} = 1700$ MPa and $\tau = 13$ years (which is time elapsed between the initial cable tensioning and the monitoring campaign). Geometrical and mechanical data for the stay cables have been reported by Mazzeo et al. [32]. Figs. 16–17 show the ratio between the natural frequency of the cables estimated by means of the proposed identification procedure $\nu_{n,\mathrm{EFD}}$ and the corresponding reference numerical values predicted by means of Eqs. (18)–(19) $\nu_{n,\mathrm{num}}$. These plots demonstrate a very good agreement between experimental values and numerical predictions. The maximum relative difference is about 5%, and a small scattering is observed by processing different records. For almost all the cables, numerical predictions of the natural frequencies are slightly larger than the experimental values.

To further confirm the accuracy of the identified natural frequency values, all records have been also processed through the VMD technique by implementing the procedure proposed by Mazzeo et al. [32] (the corresponding natural frequency values are denoted as $\nu_{n,\mathrm{VMD}}$). Results in Fig. 18 demonstrates that there exist an excellent agreement on average between the two approaches, as the points settle down close to the quadrant bisector line for both roadway directions and for all the cables. Nonetheless, a more comprehensive statistical analysis performed on the natural frequencies obtained for each cable from all available records confirms that the proposed identification approach based on the EFD technique is more robust. In fact, the maximum coefficient of variation of the natural frequencies identified by means of the EMD technique and the VMD technique is equal to $7.72 \cdot 10^{-3}$ and $6.47 \cdot 10^{-2}$, respectively.

The application of the proposed identification approach on the free vibration response of the bridge cables also allowed the modal damping ratios identification up to the fourth vibration mode. The estimated values of the modal damping ratios are listed in Table 9 (modal damping ratio values are averaged over all the available signals for the examined cable), and they are in line with typical values found in other studies about stay-cabled structures [48].

Two alternative approaches are implemented in the attempt to validate the experimental estimates of the modal damping ratios obtained by means of the proposed procedure. Particularly, free vibration responses are elaborated by means of the VMD technique following the procedure proposed by Mazzeo et al. [32]. Moreover, the cables response due to ambient vibrations are also considered to estimate their modal damping ratios using the Natural Excitation Technique (NExT) [49] combined with the area-based approach. Figs. 19–20 illustrate the modal damping ratios estimated by means of all these methods. It is remarked that it would be ideal to compare the results obtained by means of the proposed approach with those carried out from forced vibrations induced by gauged impact hammers or shakers. However, it was not possible to perform none of such vibration tests. Since the ground truth of the modal parameters is not known in real structures, the comparison of alternative approaches makes it possible to evaluate qualitatively the confidence level about the final estimates. The reasonable agreement among the modal damping ratio values that can be inferred from Figs. 19–20 substantiates the general correctness of the proposed procedure based on the EFD technique. Furthermore, it can be noted that the experimental estimates of the modal damping ratios obtained under ambient vibrations are, in most cases, slightly larger than those calculated from free vibration tests (both using the EFD technique or the VMD technique). The variability of the modal damping ratios estimated for each cable from all available records further confirms the superior robustness of the proposed identification approach based on the EFD technique for free vibrations-based dynamic identification. In fact, the maximum coefficient of variation of the modal damping ratios estimated by means of the EMD technique and the VMD technique is equal to 0.40 and 0.70, respectively.

5. Experimental application on a railway bridge

The last experimental application of the proposed identification framework deals with a typical steel bridge of the Italian railway network (Fig. 21). It is a symmetric simply supported truss bridge made up of two lateral spans, each one having length 28.54 m, and a central span whose length is 34.72 m. The bridge consists of two longitudinal truss girders spaced at 5 m, with transverse frame at the deck. Each truss girder consists of riveted longitudinal parallel top and bottom chords, struts and diagonals. Lower chords are inverse T-shaped sections, diagonals and upper chords are C-shaped built-up elements with stiffening brackets, while the struts have I-section. At the lower chords, the trusses are connected by transverse elements and cross bracing systems.

This experimental application aims at identifying natural frequencies, modal damping ratios and mode shapes of one of the lateral

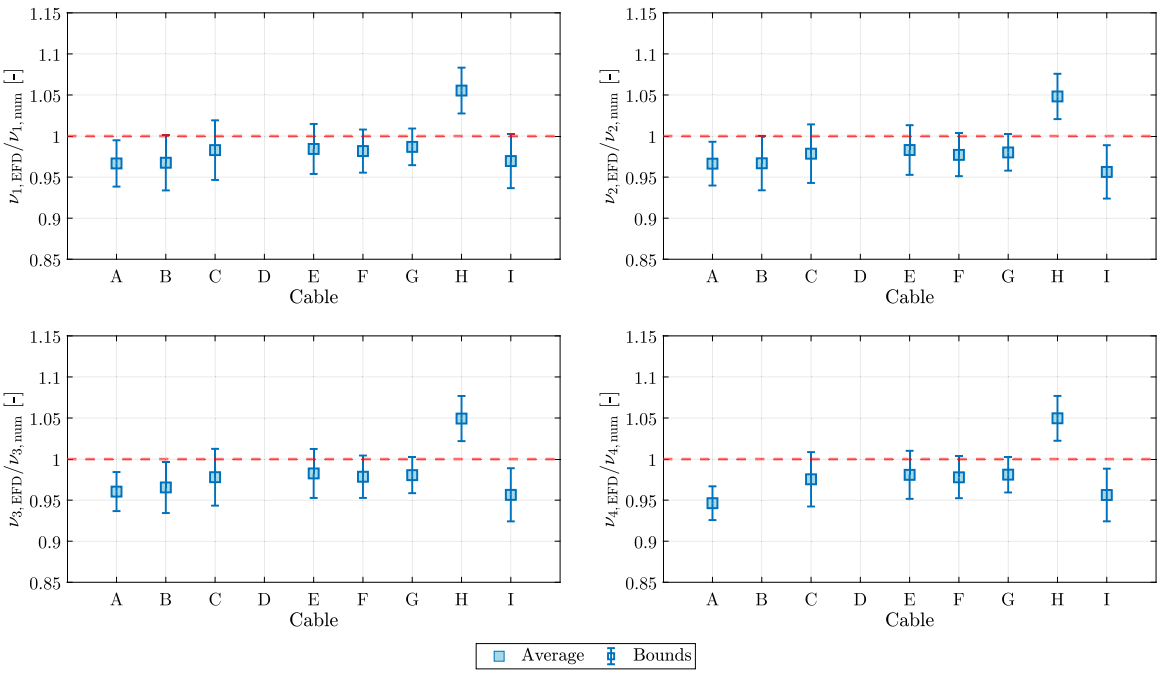

Fig. 16. Ratio between the natural frequencies of the bridge cables (Rome direction) estimated by means of the proposed identification procedure based on the EFD technique and the corresponding reference numerical values predicted by taking into account the tension losses due to steel relaxation.

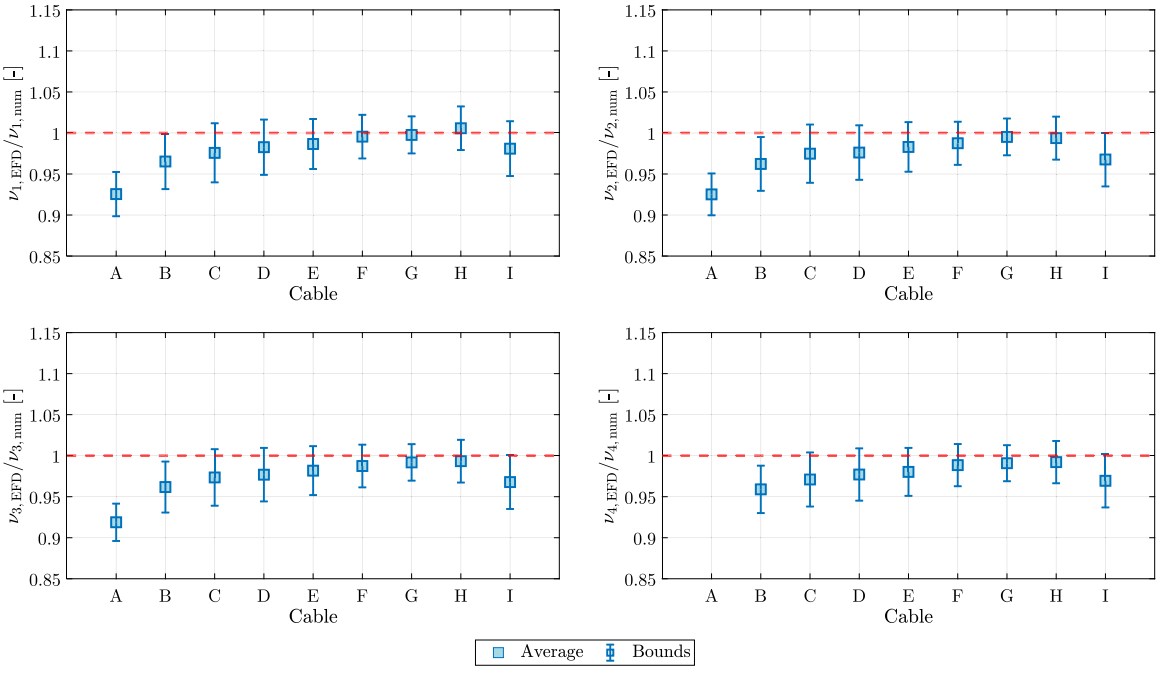

Fig. 17. Ratio between the natural frequencies of the bridge cables (Naples direction) estimated by means of the proposed identification procedure based on the EFD technique and the corresponding reference numerical values predicted by taking into account the tension losses due to steel relaxation.

spans of the investigated railway bridge from its dynamic response. Six triaxial accelerometers with sensitivity of 1000 mV/g have been installed on the deck. The accelerometers have been placed on both sides of the deck at 1/4, 1/2 and 3/4 of the span (Fig. 22). The signal acquisition was performed considering a sampling frequency $F_s = 1.6$ kHz.

The dynamic identification of the bridge is performed by exploiting its free vibrations after the passage of the train. Notably, one dataset consisting of six recordings, one for each sensor installed on the bridge deck, has been exploited to carry out the dynamic identification of the deck. Furthermore, the excitation for the present experimental application has been produced by a high-speed Frecciarossa train with a total length of 317.84 m and a gross weight of 6086.6 kN marching at an average speed equal to 163 km/h. Each recorded signal has been filtered by means of a 3rd order Butterworth band-pass filter in order to limit the analysis of the frequency range of interest, namely 3–30 Hz. The free vibration part of each signal is employed for the present analysis (Fig. 23), and it is extracted automatically according to the guidelines proposed by Yang et al. [14].

Table 9
Modal damping ratios for the first four vibration modes of the bridge cables estimated by means of the proposed procedure based on the EFD technique.

Cable	Rome direction				Naples direction			
	ξ_1 [%]	ξ_2 [%]	ξ_3 [%]	ξ_4 [%]	ξ_1 [%]	ξ_2 [%]	ξ_3 [%]	ξ_4 [%]
A	0.12	0.15	0.21	0.22	0.23	0.27	0.30	–
B	0.19	0.17	0.23	–	0.16	0.33	0.28	0.32
C	0.12	0.14	0.12	0.18	0.19	0.11	0.10	0.13
D	–	–	–	–	0.28	0.11	0.10	0.13
E	0.26	0.14	0.14	0.13	0.1	0.08	0.09	0.08
F	0.22	0.08	0.07	0.17	0.29	0.17	0.13	0.14
G	0.22	0.09	0.14	0.11	0.12	0.13	0.11	0.09
H	0.11	0.21	0.15	0.12	0.12	0.60	0.07	0.15
I	0.17	0.18	0.09	0.1	0.09	0.09	0.14	0.10

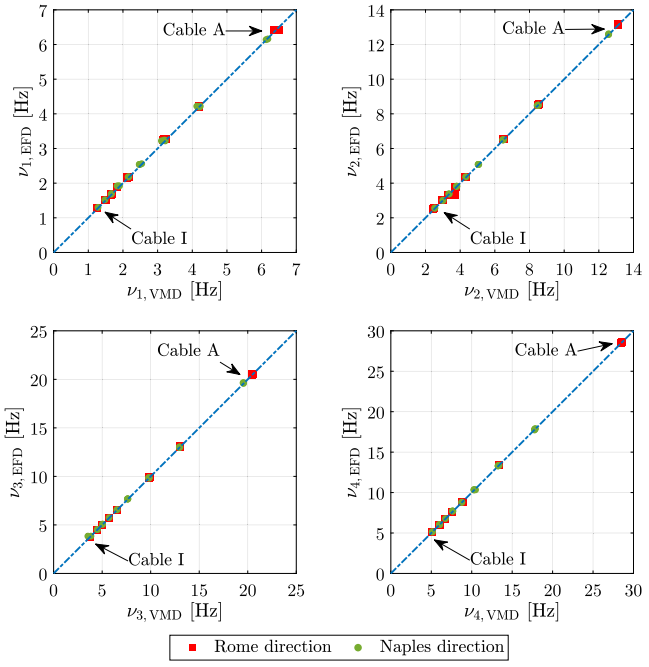

Fig. 18. Comparison of the natural frequencies of the bridge cables estimated by means of the VMD technique and EFD technique.

The modal characteristics of the monitored span of the railway bridge have been estimated by means of the proposed procedure based on the EFD technique. For the validation of these results, two further methods have been adopted to estimate the modal properties of the railway bridge. Once again, the VMD technique has been employed following the procedure described by Mazzeo et al. [32]. Moreover, the covariance-based stochastic subspace identification (SSI-COV) is adopted[1] [50,51] since the free vibration responses are proportional to the correlations of the responses to a white noise excitation [52]. Three vibration modes have been identified using all the considered techniques. The natural frequencies (average values over all the available signals) are shown Fig. 24 and demonstrate a very good agreement among the considered techniques. The statistical analysis performed on the natural frequencies obtained from each measurement point demonstrates that the proposed identification approach based on the EFD technique turns out to be more robust than that based on the VMD technique. In fact, the maximum coefficient of variation of the natural frequencies identified by means of the EMD technique and the VMD technique is $4.2 \cdot 10^{-3}$ and $1.3 \cdot 10^{-2}$, respectively. It is worth noting that the first and the second natural frequency are close to each other. This is an impediment to an accurate modal identification based on signal components extraction through a bank of band-pass filters with user-defined cut-off frequencies, as usual in common practice. The identified mode shapes are illustrated in Fig. 25. First and third vibration modes are representative of vertical flexural mode shapes (first and second bending mode, respectively) whereas the second vibration mode corresponds to a torsional mode shape. Fig. 25 also provides a comparison between the mode shapes identified through the proposed approach based on the EFD technique and those obtained through the SSI-COV method. The Modal Assurance Criterion (MAC) can be employed to assess quantitatively the agreement between the mode shapes carried out by means of these two alternative approaches (i.e., the closer MAC is to 1, the higher the similarity between the mode shapes carried out via EFD technique and the SSI-COV method). As regards the considered railway bridge deck, a MAC value equal to 0.95, 0.97 and 0.94 for the first, second and third mode has been found, respectively. Therefore, the mode shapes obtained by means of the procedure proposed in the present work agree very well with those estimated through the SSI-COV technique. This confirms that the proposed procedure based on the EFD technique identifies accurately the mode shapes, with a much lower computational effort than the SSI-COV technique. Indeed, some operations invoked into the SSI-COV technique (such as the preparation of the block Toeplitz matrix of covariances and the singular value decomposition) need a high elaboration time and a large memory usage while the implementation of the proposed approach requires basic operations and a minimum computational effort.

Fig. 26 is meant at comparing the modal damping ratios obtained by means of the considered alternative identification methods. The results in Fig. 26 demonstrate a general good agreement between the estimates obtained by means of the proposed approach and those carried out via the VMD technique. There is, however, a rather significant difference about the modal damping ratio value for the third vibration mode, as estimated at some measurement points. The statistical elaboration of the modal damping ratios obtained from different measurement points further confirms the large robustness of the dynamic identification performed according to the approach presented in the current study. While the maximum coefficient of variation of the modal damping ratios identified by means of the proposed approach is 0.36, the corresponding value obtained via VMD technique is equal to 0.42.

For the sake of completeness, it is pointed that the modal damping ratios estimated via SSI-COV technique are $\xi_1 = 2.3\%$, $\xi_2 = 2.5\%$ and $\xi_3 = 1.4\%$. Hence, the first and the third modal damping ratio values differ significantly from those calculated through the EFD technique and the VMD technique. Actually, this difference is attributable to the fact that SSI methods are not always able to identify accurately the damping ratios in case of strongly non-stationary signals [53].

For a critical examination of the obtained estimates of the modal damping ratios, reference values from relevant technical codes and reports are considered. In this regard, Eurocode 1- Part 2 §6.4.6.3.1 [54] provides the lower bound value of the modal damping ratio, which is assumed constant for all modes and is based on the construction

[1] The identification by means of the SSI-COV technique is performed using the open-source toolkit available at https://code.vt.edu/vibes-lab/modal-analysis.

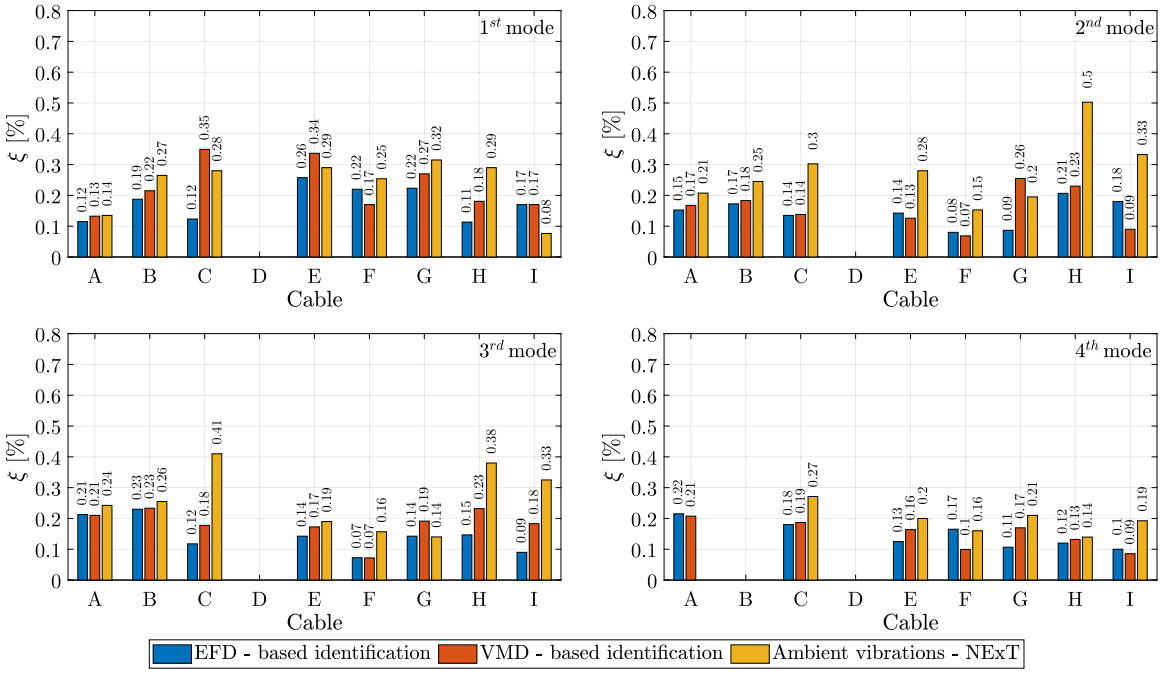

Fig. 19. Modal damping ratios for the first four vibration modes of the bridge cables (Rome direction) estimated by means of the proposed procedure based on the EFD technique and two alternative methods.

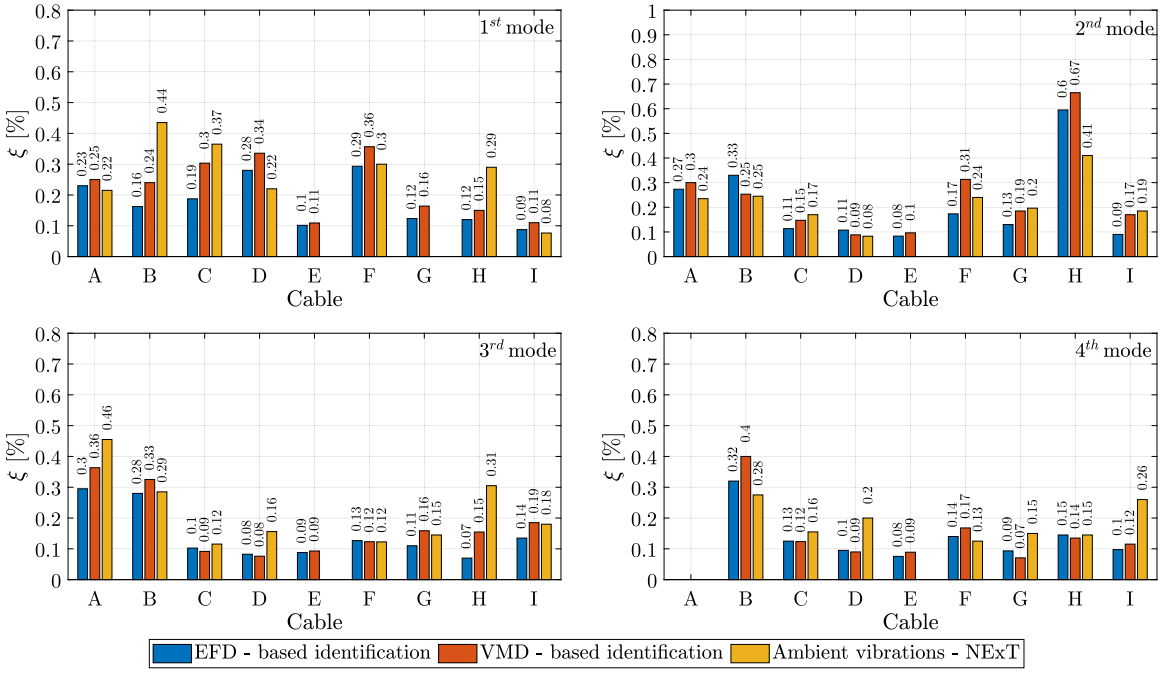

Fig. 20. Modal damping ratios for the first four vibration modes of the bridge cables (Naples direction) estimated by means of the proposed procedure based on the EFD technique and two alternative methods.

Table 10
Lower limit of the modal damping ratio proposed in EC1 – Part 2 [54].

Bridge type	Lower limit of percentage of critical damping [%]	
	Span $L < 20$ m	Span $L > 20$ m
Steel and composite	$\xi = 0.5 + 0.125(20 - L)$	$\xi = 0.5$
Prestressed concrete	$\xi = 1 + 0.07(20 - L)$	$\xi = 1$
Filler beam and reinforced concrete	$\xi = 1.5 + 0.07(20 - L)$	$\xi = 1.5$

Fig. 21. Overview of steel railway bridge investigated in the present work.

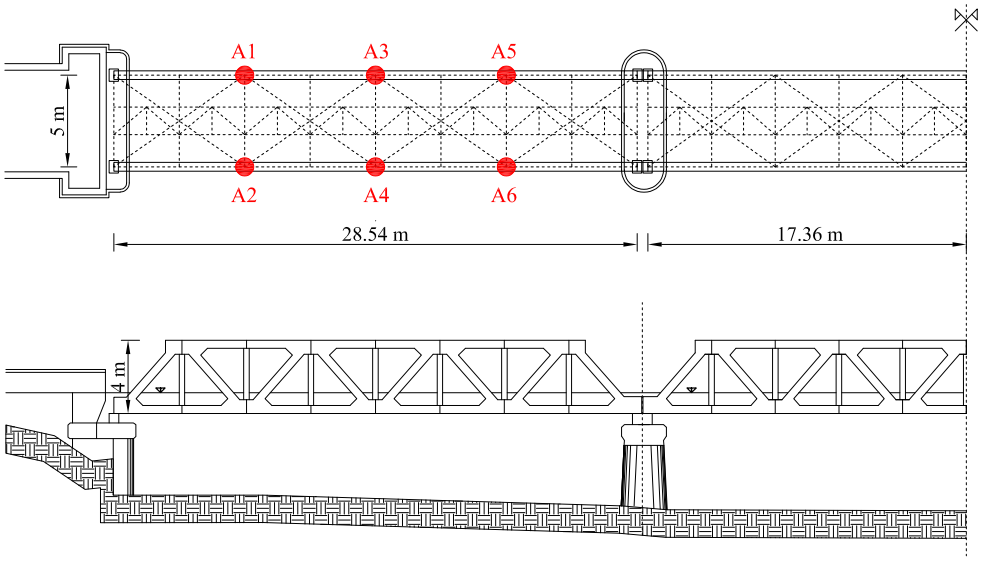

Fig. 22. Layout of the steel railway bridge and details about the sensors position for monitoring the dynamic response of one lateral span.

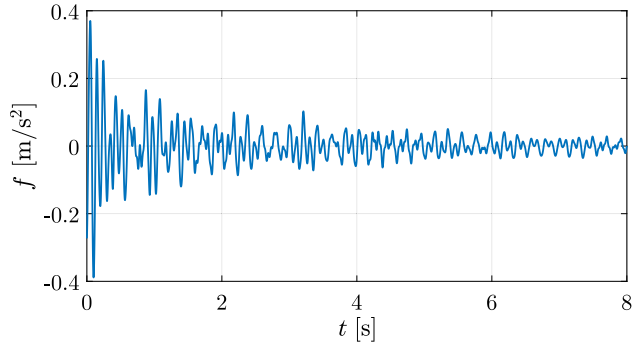

Fig. 23. Free vibration part extracted from a recorded acceleration signal of the steel railway bridge.

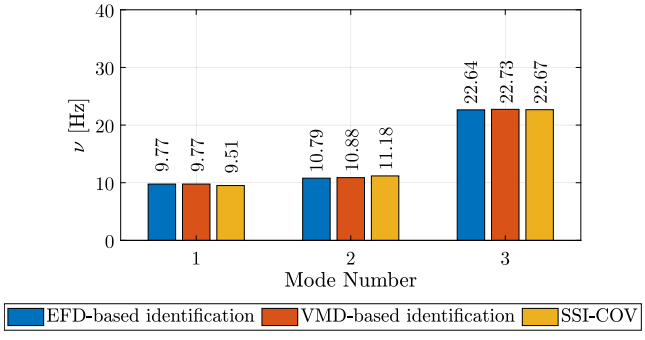

Fig. 24. Natural frequencies of the railway bridge span estimated according to different identification methods.

material of the bridge as well as on the span length, as reported in Table 10.

Another estimation of the damping ratio is provided by the European Commission in the "Guideline for estimating structural damping of railway bridges" D5.2-S2 [55]. In this case, the constant modal damping ratio can be calculated as the sum of three different contributions depending on the specifics of the structure, namely material, structural type and bearings type. Table 11 lists the contributions as named in such guideline for this specific case.

Table 11
Modal damping ratio value proposed in D5.2-S2 [55].

	Damping ratio [%]
Material damping: steel	0.08
Nonmaterial structural damping: steel riveted bridge	0.32
Interaction damping: standard sliding bearings	0.24

For the examined case study, a constant minimum value of the modal damping ratio equal to $\xi = 0.5\%$ is recommended by Eurocode 1 – Part 2 [54] while a constant modal damping ratio $\xi = 0.64\%$ is calculated following the guidelines into D5.2-S2 [55]. It can be thus

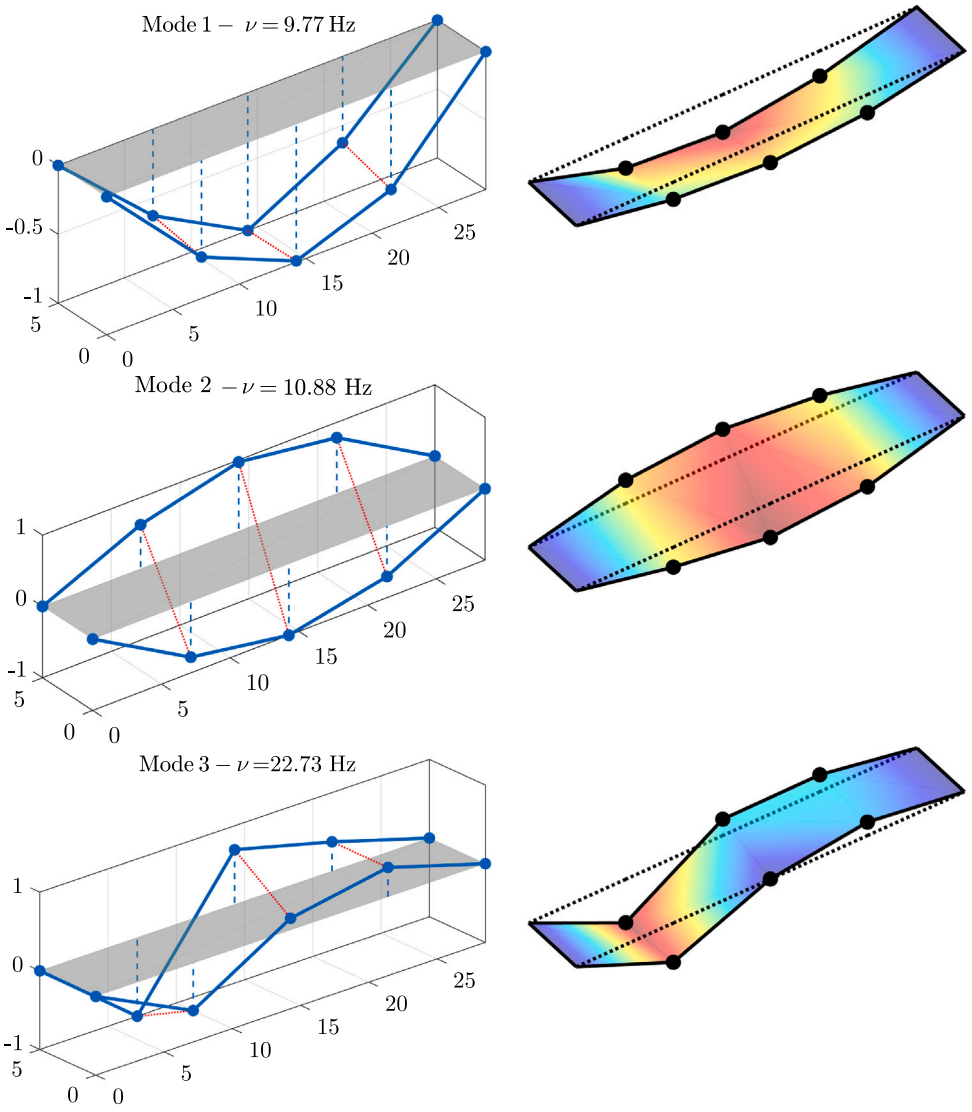

Fig. 25. Estimated mode shapes of the railway bridge span: identification by means of the proposed approach based on EFD technique (left); identification by means of the SSI-COV technique (right).

concluded that the lower bound recommended by Eurocode 1 – Part 2 as well as the constant modal damping ratio value suggested by D5.2-S2 agree well with the minimum estimates of the modal damping ratio found in the present study, which occur for the third vibration mode as shown in Fig. 26. These reference values underestimate the modal damping ratios for the first and the second vibration mode as plotted in Fig. 26, being conservative towards the actual overall dissipation capacity of the structure. Finally, it is pointed out that the estimated modal damping ratios are in reasonable agreement with the values reported in other studies [56–58] on steel truss railway bridges with similar materials and static configuration.

6. Conclusions

A novel implementation of the EFD technique has been proposed in the present work for the automatic identification of the modal parameters of structures from their free vibration response. The decomposition method has been enhanced by introducing an automatic procedure for the selection of the number of frequency partitions. The robustness of the segmentation procedure has been improved by means of a zero-phase moving average smoothing filtering of the frequency spectrum that mitigates the negative effects of noise. An area-based approach is adopted to identify the modal damping ratio for each extracted component. A time-domain method based on the phase shift of the free vibration response peaks is employed to identify the mode shapes. The proposed identification framework has been tested on numerical benchmark signals representative of the free vibration response of multi-degree-of-freedom structural systems. The proposed approach is finally applied to two real bridges, where a comparative assessment with alternative approaches is presented to further validate the proposed identification framework. The following conclusions can be drawn from the results reported within the present study.

- The statistical comparative assessment between the EFD technique and the VMD technique based on the analysis of synthetic signals demonstrates that both methods lead to very good results on average, provided that the involved control parameters are properly defined. Particularly, both techniques are able to provide an accurate identification in the case of closely spaced modes. The performance of the EFD technique and that of the VMD technique are instead dramatically different from each other when dealing with a lowly excited vibration mode. In such circumstance, it is found that the identification via VMD technique is prone to errors propagation and sometimes fails. Conversely, the proposed approach based on the implementation of the EFD technique

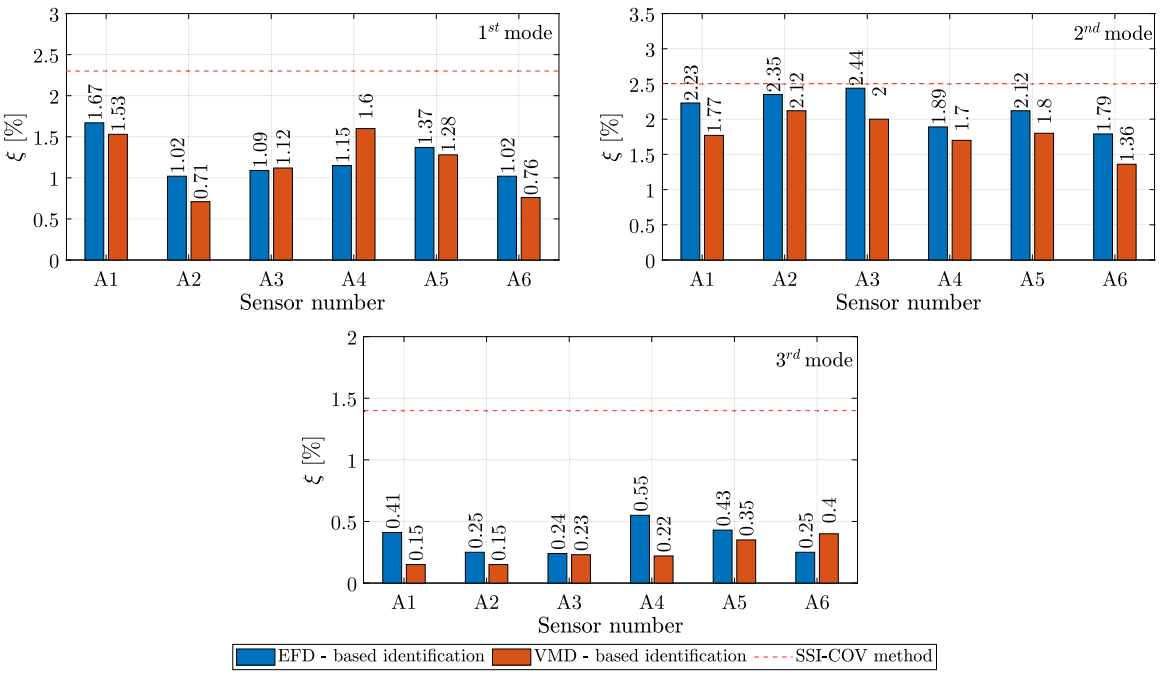

Fig. 26. Modal damping ratios of the railway bridge span estimated according to different identification methods.

exhibits much greater robustness and is able to provide satisfactory results every time. Furthermore, the implementation of the automatic procedure developed in the current work for the dynamic identification of structures via EFD technique is more straightforward than the one based on the VMD technique.

- The analysis of synthetic signals contaminated by noise also showed that the use of the standard logarithmic decrement method is not able to ensure the accurate identification of the modal damping ratios while the robust area-based approach herein implemented is crucial. Hence, regardless the adopted signal decomposition technique and its reliability, it is essential to use appropriate strategies to obtain reliable estimates of the modal damping ratio.
- The automatic procedure developed in the current work for the dynamic identification of structures via EFD technique has been successfully applied to the experimental characterization of two existing bridges. This further demonstrates its general correctness and its feasibility for practical applications. The comparison with the results obtained by means of the VMD technique also demonstrates that the proposed methodology based on the EFD technique leads to more consistent estimates of the modal parameters, thereby confirming its robustness.

CRediT authorship contribution statement

Matteo Mazzeo: Conceptualization, Methodology, Investigation, Data curation, Software, Writing – original draft, Writing – review & editing. **Dario De Domenico:** Conceptualization, Methodology, Investigation, Data curation, Software, Formal analysis, Visualization, Validation, Writing – review & editing. **Giuseppe Quaranta:** Conceptualization, Methodology, Investigation, Formal analysis, Software, Writing – review & editing, Supervision, Funding acquisition. **Roberta Santoro:** Conceptualization, Methodology, Investigation, Writing – review & editing.

Declaration of competing interest

The authors declare that they have no known competing financial interests or personal relationships that could have appeared to influence the work reported in this paper.

Data availability

The data that has been used is confidential.

Acknowledgments

The authors would like to thank the two anonymous reviewers for their valuable comments and suggestions. The work of Giuseppe Quaranta was carried out within the RETURN Extended Partnership funded by the European Union Next – GenerationEU (National Recovery and Resilience Plan – NRRP, Mission 4, Component 2, Investment 1.3 – D.D. 1243 2/8/2022, PE0000005).

References

[1] Ereiz S, Duvnjak I, Jiménez-Alonso JF. Review of finite element model updating methods for structural applications. In: Structures, vol. 41. Elsevier; 2022, p. 684–723.
[2] Moughty JJ, Casas JR. A state of the art review of modal-based damage detection in bridges: Development, challenges, and solutions. Appl Sci 2017;7(5).
[3] Magalhães F, Cunha Á, Caetano E, Brincker R. Damping estimation using free decays and ambient vibration tests. Mech Syst Signal Process 2010;24(5):1274–90.
[4] Braga F, Laterza M. Field testing of low-rise base isolated building. Engineering structures 2004;26(11):1599–610.
[5] Oliveto ND, Scalia G, Oliveto G. Time domain identification of hybrid base isolation systems using free vibration tests. Earthq Eng Struct Dyn 2010;39(9):1015–38.
[6] Athanasiou A, Oliveto ND, Ponzo FC. Identification of first and second order models for the superstructure of base-isolated buildings using free vibration tests: A case study. Soil Dyn Earthq Eng 2020;135:106178.
[7] Shi W, Shan J, Lu X. Modal identification of Shanghai World Financial Center both from free and ambient vibration response. Eng Struct 2012;36:14–26.
[8] Ivorra S, Pallarés FJ. Dynamic investigations on a masonry bell tower. Eng Struct 2006;28(5):660–7.
[9] Lagomarsino S, Calderini C. The dynamical identification of the tensile force in ancient tie-rods. Eng Struct 2005;27(6):846–56.
[10] Binda L, Cantini L, Tiraboschi C, Amigoni C, et al. Non destructive investigation for the conservation design of a monastery near Bergamo (Italy). In: RILEM symposium on on site assessment of concrete, masonry and timber structures. RILEM Publications SARL; 2008, p. 797–806.
[11] Cunha A, Caetano E, Delgado R. Dynamic tests on large cable-stayed bridge. J Bridge Eng 2001;6(1):54–62.

[12] Magalhães F, Caetano E, Cunha Á, Flamand O, Grillaud G. Ambient and free vibration tests of the Millau viaduct: Evaluation of alternative processing strategies. Eng Struct 2012;45:372–84.
[13] Lorenzoni F, De Conto N, da Porto F, Modena C. Ambient and free-vibration tests to improve the quantification and estimation of modal parameters in existing bridges. J Civ Struct Health Monit 2019;9:617–37.
[14] Yang X-M, Yi T-H, Qu C-X, Li H-N, Liu H. Modal identification of high-speed railway bridges through free-vibration detection. J Eng Mech 2020;146(9):04020107.
[15] Ko JM, Zheng G, Chen Z, Ni Y-Q. Field vibration tests of bridge stay cables incorporated with magnetorheological (MR) dampers. In: Smart structures and materials 2002: Smart systems for bridges, structures, and highways, vol. 4696. 4696, SPIE; 2002, p. 30–40.
[16] Van Nimmen K, Van den Broeck P, Gezels B, Lombaert G, De Roeck G. Experimental validation of the vibration serviceability assessment of a lightweight steel footbridge with tuned mass damper. In: Proc., ISMA 2012 int. conf. on noise and vibration engineering. 2012, p. 1145–58.
[17] Huang NE, Shen Z, Long SR, Wu MC, Shih HH, Zheng Q, et al. The empirical mode decomposition and the Hilbert spectrum for nonlinear and non-stationary time series analysis. Proc R Soc Lond Ser A Math Phys Eng Sci 1998;454(1971):903–95.
[18] Wu Z, Huang NE. Ensemble empirical mode decomposition: a noise-assisted data analysis method. Adv Adapt Data Anal 2009;1(01):1–41.
[19] Yang W, Peng Z, Wei K, Shi P, Tian W. Superiorities of variational mode decomposition over empirical mode decomposition particularly in time–frequency feature extraction and wind turbine condition monitoring. IET Renew Power Gener 2017;11(4):443–52.
[20] Xu B, Sheng Y, Li P, Cheng Q, Wu J. Causes and classification of EMD mode mixing. Vibroengineering Procedia 2019;22:158–64.
[21] Feldman M. Time-varying vibration decomposition and analysis based on the Hilbert transform. J Sound Vib 2006;295(3–5):518–30.
[22] Gilles J. Empirical wavelet transform. IEEE Trans. Signal Process. 2013;61(16):3999–4010.
[23] Hu Y, Li F, Li H, Liu C. An enhanced empirical wavelet transform for noisy and non-stationary signal processing. Digit Signal Process 2017;60:220–9.
[24] Zhou W, Feng Z, Xu Y, Wang X, Lv H. Empirical Fourier decomposition: An accurate signal decomposition method for nonlinear and non-stationary time series analysis. Mech Syst Signal Process 2022;163:108155.
[25] Singh P, Joshi SD, Patney RK, Saha K. The Fourier decomposition method for nonlinear and non-stationary time series analysis. Proc R Soc A 2017;473(2199):20160871.
[26] Kizilkaya A, Elbi MD. A fast approach of implementing the Fourier decomposition method for nonlinear and non-stationary time series analysis. Signal Process 2023;206:108916.
[27] Dragomiretskiy K, Zosso D. Variational mode decomposition. IEEE Trans Signal Process 2013;62(3):531–44.
[28] Bagheri A, Ozbulut OE, Harris DK. Structural system identification based on variational mode decomposition. J Sound Vib 2018;417:182–97.
[29] Civera M, Surace C. A comparative analysis of signal decomposition techniques for structural health monitoring on an experimental benchmark. Sensors 2021;21(5):1825.
[30] Gong W-B, Li A, Wu Z-H, Qina F-J. Nonlinear vibration feature extraction based on power spectrum envelope adaptive empirical Fourier decomposition. ISA Trans 2023.
[31] Mazzeo M, De Domenico D, Quaranta G, Santoro R. A novel procedure for damping ratio identification from free vibration tests with application to existing bridge decks. In: European workshop on structural health monitoring: EWSHM 2022-Volume 3. Springer; 2022, p. 699–708.
[32] Mazzeo M, De Domenico D, Quaranta G, Santoro R. Automatic modal identification of bridges based on free vibration response and variational mode decomposition technique. Eng Struct 2023;280:115665.
[33] Santoshkumar B, Khasawneh FA. Guidelines for optimizing the error in area ratio damping estimation method. In: Yu L, Untaroiu C, Munoz L, editors. Proceedings of the ASME 2021 international design engineering technical conferences and computers and information in engineering conference. ASME; 2021.
[34] Shi P, Yang W, Sheng M, Wang M. An enhanced empirical wavelet transform for features extraction from wind turbine condition monitoring signals. Energies 2017;10(7):972.
[35] Xu Y, Deng Y, Zhao J, Tian W, Ma C. A novel rolling bearing fault diagnosis method based on empirical wavelet transform and spectral trend. IEEE Trans Instrum Meas 2019;69(6):2891–904.
[36] Azami H, Mohammadi K, Bozorgtabar B. An improved signal segmentation using moving average and Savitzky-Golay filter. J Signal Inf Process 2012;39–44.
[37] Luo J, Ying K, Bai J. Savitzky–Golay smoothing and differentiation filter for even number data. Signal Process 2005;85(7):1429–34.
[38] Betta G, Capriglione D, Cerro G, Ferrigno L, Miele G. The effectiveness of savitzky-golay smoothing method for spectrum sensing in cognitive radios. In: 2015 XVIII AISEM annual conference. IEEE; 2015, p. 1–4.
[39] Papoulis A. Random variables and stochastic processes. McGraw Hill; 1991.
[40] Li S, Liu Y, Wang P, Li X, Li Z. Modal parameter identification for closely spaced modes using an Empirical Fourier decomposition-based method. Sci Iran 2022.
[41] Au S-K, Brownjohn JM, Li B, Raby A. Understanding and managing identification uncertainty of close modes in operational modal analysis. Mech Syst Signal Process 2021;147:107018.
[42] Liang T, Lu H, Sun H. Application of parameter optimized variational mode decomposition method in fault feature extraction of rolling bearing. Entropy 2021;23(5):520.
[43] He X, Hua X, Chen Z, Huang F. EMD-based random decrement technique for modal parameter identification of an existing railway bridge. Eng Struct 2011;33(4):1348–56.
[44] Maruccio C, Quaranta G, De Lorenzis L, Monti G. Energy harvesting from electrospun piezoelectric nanofibers for structural health monitoring of a cable-stayed bridge. Smart Mater Struct 2016;25(8):085040.
[45] Clemente P, Marulo F, Lecce L, Bifulco A. Experimental modal analysis of the Garigliano cable-stayed bridge. Soil Dyn Earthq Eng 1998;17(7–8):485–93.
[46] Fang Z, Wang J-q. Practical formula for cable tension estimation by vibration method. J Bridge Eng 2012;17(1):161–4.
[47] Code P. Eurocode 2: design of concrete structures-part 1-1: general rules and rules for buildings. London: British Standard Institution; 2005.
[48] Chen C-C, Wu W-H, Yu S-T, Lai G. Investigation of modal damping ratios for stay cables based on stochastic subspace identification with ambient vibration measurements. Adv Struct Eng 2019;22(16):3444–60.
[49] James III GH, Carne TG, Lauffer JP. The natural excitation technique (NExT) for modal parameter extraction from operating wind turbines. Tech. rep., Albuquerque, NM (United States): Sandia National Labs.; 1993.
[50] Peeters B, De Roeck G. Reference-based stochastic subspace identification for output-only modal analysis. Mech Syst Signal Process 1999;13(6):855–78.
[51] Van Overschee P, De Moor B. Subspace identification for linear systems: Theory—implementation—applications. Springer Science & Business Media; 2012.
[52] Magalhães F, Caetano E, Cunha Á. Operational modal analysis of the braga sports stadium suspended roof. In: Proceedings of the 24th IMAC. 2006.
[53] Li W, Vu V-H, Liu Z, Thomas M, Hazel B. Extraction of modal parameters for identification of time-varying systems using data-driven stochastic subspace identification. J Vib Control 2018;24(20):4781–96.
[54] Eurocode 1: Actions on structures — Part 2: Traffic loads on bridges. EN1991-2. London: British Standard Institution; 2003.
[55] Feltrin G, Sedlacek G, Soorensen R, Froolund T, Luczynski B. Monitoring guidelines for railway bridges, SB-MON: sustainable bridges guideline, sb d5. 2. 2007.
[56] Bacinskas D, Kamaitis Z, Jatulis D, Kilikevicius A. Field testing of old narrow-gauge railway steel truss bridge. Procedia Eng 2013;57:136–43.
[57] Gattulli V, Lofrano E, Paolone A, Potenza F. Measured properties of structural damping in railway bridges. J Civ Struct Health Monit 2019;9:639–53.
[58] Venglár M, Lamperová K, Sokol M. Performance assessment of steel truss railway bridge with curved track. Acta Polytech 2022;62(5):558–66.